Interannual variability of Great Lakes ice cover and its relationship to NAO and ENSO

Xuezhi Bai,[1] Jia Wang,[2] Cynthia Sellinger,[3] Anne Clites,[2] and Raymond Assel[1,2]

[1]   The impacts of North Atlantic Oscillation (NAO) and El Niño–Southern Oscillation (ENSO) on Great Lakes ice cover were investigated using lake ice observations for winters 1963–2010 and National Centers for Environmental Prediction reanalysis data. It is found that both NAO and ENSO have impacts on Great Lakes ice cover. The Great Lakes tend to have lower (higher) ice cover during the positive (negative) NAO. El Niño events are often associated with lower ice cover. The influence of La Niña on Great Lakes ice cover is intensity-dependent: strong (weak) La Niña events are often associated with lower (higher) ice cover. The interference of impacts of ENSO and NAO complicates the relationship between ice cover and either of them. The nonlinear effects of ENSO on Great Lakes ice cover are important in addition to NAO effects. The correlation coefficient between the quadratic Nino3.4 index and ice cover (-0.48) becomes significant at the 99% confidence level. The nonlinear response of Great Lakes ice cover to ENSO is mainly due to the phase shift of the teleconnection patterns during the opposite phases of ENSO. Multiple-variable nonlinear regression models were developed for ice coverage. Using the quadratic Nino3.4 index instead of the index itself can significantly improve the prediction of Great Lakes ice cover (the correlation between the modeled and observed increases from 0.35 to 0.51). Including the interactive term NAO·Nino3.4^2 further improves the prediction skill (the correlation increases from 0.51 to 0.59). The analysis is also applied to individual lakes. The model for Lake Michigan has the highest prediction skill, while Lake Erie has the smallest skill.

1. Introduction

[2]   The Laurentian Great Lakes, located in the midlatitude of eastern North America, contain about 95% of the U.S. and 20% of the world's fresh surface water supply. The ice cover that forms on the Great Lakes each winter affects the regional economy [*Niimi*, 1982], the Lakes' ecosystem [*Vanderploeg et al.*, 1992; *Brown et al.*, 1993; *Magnuson et al.*, 1995], the water balance, and the water level variability [*Assel et al.*, 2004]. The presence (or absence) of ice cover on lakes during the winter months is also known to have significant effects on both regional climate and weather events (such as thermal moderation and lake effect snow) [*Brown and Duguay*, 2010]. Lake ice cover is a sensitive indicator of regional climate and climate change [*Smith*,

1991; *Hanson et al.*, 1992; *Assel and Robertson*, 1995; *Assel et al.*, 2003; *Wang et al.*, 2012]. Seasonal ice cover repeats from year to year but has a large interannual variability. For example, the maximum ice coverage was 95% in 1979 and only 11% in 2002. The relationship between air temperature and ice phenology is well established [*Bilello*, 1980; *Palecki and Barry*, 1986; *Williams*, 1965] whereby the preceding air temperature, for weeks to months depending on the location, can be used as a predictor of freezeup/breakup. In the North Hemisphere, freezeup in northern areas (e.g., Lake Kallavesi, Finland) reflects the climate conditions around October and November, while freezeup in areas further south (e.g., Grand Traverse Bay, Lake Michigan) reflects the climate from January to February [*Magnuson et al.*, 2000].

[3] Studies showed that teleconnection patterns such as the Pacific/North America (PNA) [*Wallace and Gutzler*, 1981] (Figure 1a), North Atlantic Oscillation (NAO) (Figure 1b), Pacific Decadal Oscillation (PDO), and West Pacific (WP), are associated with anomalous ice cover on the Great Lakes [*Assel and Rodionov*, 1998; *Rodionov and Assel*, 2000, 2003; *Rodionov et al.*, 2001] and other small lakes in North America [*Anderson et al.*, 1996; *Robertson et al.*, 2000; *Bonsal et al.*, 2006; *Mishra et al.*, 2011]. *Assel*

---

[1]Cooperative Institute for Limnology and Ecosystems Research, University of Michigan, Ann Arbor, Michigan, USA.
[2]Great Lakes Environmental Research Laboratory, NOAA, Ann Arbor, Michigan, USA.
[3]College of Oceans and Atmospheric Sciences, Oregon State University, Corvallis, Oregon, USA.

PNA

NAO
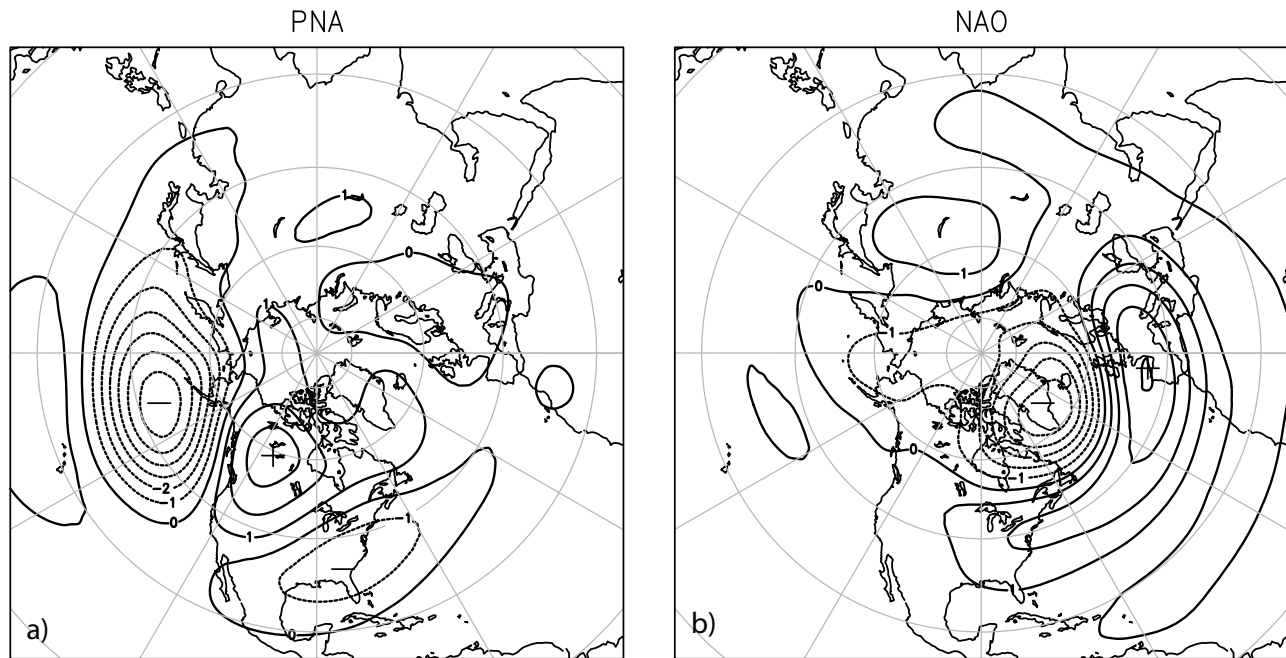
Figure 1. The positive phase of (a) PNA and (b) NAO patterns (interval: 1dam). The pattern was obtained by regressing the PNA and NAO index upon the winter mean 500 hPa geopotential height anomaly for the period 1951–2010.

and Rodionov [1998] pointed out that ice cover on the Great Lakes tends to be below average during El Niño events, but association between La Niña events and above-average ice cover in the Great Lakes basin is much weaker and less stable. Ice-off dates for Lake Mendota, Wisconsin, have been associated with El Niño events [*Anderson et al.*, 1996; *Robertson et al.*, 2000]. The observed changes in Canada's lake ice cover have also been influenced by large-scale atmospheric teleconnections [*Bonsal et al.*, 2006]. Ice phenology was shown to be more responsive to the extreme phases of the teleconnections, with the Pacific indices (PNA, PDO, SOI and NP) having the strongest correlation to ice cover, with the exception of the extreme eastern areas, which were more affected by NAO [*Bonsal et al.*, 2006]. A recent study [*Mishra et al.*, 2011] also shows that lake ice phenology of small lakes around the Great Lakes region is associated with these major climate teleconnection patterns, including NAO, AO (Arctic Oscillation), and AMO (Atlantic Multidecadal Oscillation). *Assel and Rodionov* [1998] also found that the negative mode of the NAO appears to be associated with above-average ice cover on the Great Lakes. *Livingstone* [2000] found that the NAO signal in the ice phenology records from Lake Mendota was present and strong from the latter half of the nineteenth century to the first half of the twentieth century but had weakened since then. *Ghanbari et al.* [2009] found that the ice cover on Lake Mendota was affected at the interannual and interdecadal scale by teleconnections; most prominently by the effects of PDO (through snowfall/snow depth) and SOI (through temperature) at the interannual scale and by the PDO (through air temperature) and NAO (through snowfall) at the interdecadal scale.

[4] Researchers documented ENSO signals in North American temperature since the 1980s [*Ropelewski and*

Halpert, 1986; *Kiladis and Diaz*, 1989; *Halpert and Ropelewski*, 1992; *Gershunov and Barnett*, 1998]. The well-known pattern associated with El Niño, features above-normal surface air temperature (SAT) along the west coast of North America and in western and central Canada; and below-normal SAT in the southern tier of the U.S. and the Gulf of Mexico. This distribution of SAT anomalies is often explained by the PNA type of atmospheric circulation excited during El Niño events. Recent evidence from observational studies and numerical models showed that North America surface temperature has asymmetric response patterns during the opposite phases of ENSO [*Livezey et al.*, 1997; *Hoerling et al.*, 1997, 2001; *Wu et al.*, 2005]. Using neural networks, *Wu et al.* [2005] examined the nonlinear patterns of the North America winter temperature associated with ENSO. They found that the Great Lakes are located in the strong impact region by the nonlinear component of the ENSO, making this region particularly interesting for studying the mechanism of the ENSO effect on the North America climate and lake ice variability.

[5] The extratropical atmospheric response to El Niño in the northern winter is mainly manifested by the PNA teleconnection pattern [*Wallace and Gutzler*, 1981; *Horel and Wallace*, 1981] (Figure 1a). The PNA pattern accounts for a considerable part of the variance of interannual climate fluctuations over the North Pacific and North America and is regarded as a major source of skill for seasonal forecast [e.g., *Zwiers*, 1987; *Barnston*, 1994; *Shabbar and Barnston*, 1996; *Derome et al.*, 2001].

[6] Besides the PNA, the Tropical Northern Hemisphere (TNH), WP, and North Pacific (NP) patterns are also associated with changes in sea surface temperature (SST) in the tropical Pacific [*Mo and Livezey*, 1986; *Trenberth et al.*, 1998]. The TNH pattern was first classified by *Mo and*

Livezey [1986] and appears as a prominent wintertime mode during December–February. The positive phase of the TNH pattern features above-average heights over the Gulf of Alaska and from the Gulf of Mexico northeastward across the western North Atlantic, and below-average heights throughout eastern Canada. The PNA, WP, and TNH exist in winter, while the NP applies to the March–May season. An individual pattern, therefore, cannot reflect all of ENSO's influences.

[7] Geographically, the Great Lakes are located on the edge of two important teleconnection patterns affecting the North America climate: PNA and NAO. These two climate patterns play a very important role in interannual variability of U.S. climate. However, their impacts on Great Lakes ice cover should be marginally significant. For PNA, the Great Lakes are positioned between the Alberta High and the southeastern U.S. Low, close to the nodal point of this standing oscillation (Figure 1a). Any distortion of the pattern and shift of the centers may result in different responses in winter temperature, and thus ice cover. *Assel and Rodionov* [1998] found that annual maximum ice cover on the Great Lakes had a relatively poor association with the PNA index and, at the same time, a substantial ENSO signal. Furthermore, *Rodionov and Assel* [2000, 2001] argued that ENSO is not the only source responsible for exciting the PNA pattern. Some observational and modeling studies indicate that the atmospheric response to the extratropical sea surface temperature (SST) anomalies may be even stronger than the response to the tropical SST anomalies [*Lau and Nath*, 1990; *Wallace and Jiang*, 1992; *Wallace et al.*, 1990, 1992]. On the other hand, the PNA is not the sole pattern that occurs during ENSO events. The WP and the TNH patterns were also found to be related to ENSO [*Horel and Wallace*, 1981; *Barnston and Livezey*, 1987]. These two patterns can make a substantial difference in winter temperatures over the Great Lakes basin in response to ENSO events and the PNA.

[8] For NAO, the Great Lakes are located at the southwestern edge of the Icelandic Low and northeastern edge of the Azores High, far away from the action centers (Figure 1b). So, the NAO may have influences on the Great lakes ice cover to some degree, but are not dominant. Unlike the PNA, WP, and TNH patterns, variations in NAO appear to be relatively more independent from ENSO [*Rogers*, 1984].

[9] *Bai et al.* [2010] systematically investigated the relationships between lake ice and ENSO and AO/NAO teleconnection patterns. They found that both ENSO and NAO impact Great Lakes ice cover. In addition, the geographic location of the Great Lakes and the interference impacts of the ENSO and NAO complicate the relationship between ice cover and ENSO or NAO [*Wang et al.*, 1994; *Mysak et al.*, 1996]. This makes forecasting ice cover challenging. This paper aims to further investigate the impacts of ENSO and NAO, both individually and combined, on Great Lakes ice cover.

[10] The paper is organized as follows. The data and the methods are briefly introduced in section 2. The relationships between Great Lakes ice cover and individual NAO and ENSO events are discussed in section 3. In section 4, the combination and interference effects of ENSO and NAO are investigated in detail. Section 5 presents both linear and nonlinear regression models for hindcasting lake ice, and

section 6 shows a case study. Last, section 7 summarizes the results.

2. Data and Methods

2.1. Annual Maximum Ice Cover

[11] Systematic lake-scale observations of Great Lakes ice cover began in the 1960s by federal agencies in the U.S. (U.S. Army Corps of Engineers, U.S. Coast Guard) and Canada (Atmospheric Environment Service, Canadian Coast Guard). Ice charts depicting ice concentration patterns and ice extent were constructed from satellite imagery, side-looking airborne radar imagery, and visual aerial ice reconnaissance [*Assel and Rodionov*, 1998].

[12] Annual maximum ice coverage (AMIC) is defined as the greatest percent of surface area of a lake covered by ice each winter for the Great Lakes. The AMIC for each lake and the Great Lakes as a whole for winters 1963–2010 (Figure 2) was calculated using the data set archived at the NOAA Great Lakes Environmental Research Laboratory [*Assel et al.*, 2003]. The long-term mean and standard deviation (STD) of AMIC for each lake and the whole Great Lakes are listed in Table 1. Lake Erie, the shallowest one, has the maximum long-term mean AMIC (85%) while Lake Ontario has the minimum (24.6%). Lake Michigan has the second small AMIC (37.7%). The long-term mean AMICs in Lakes Superior and Huron are almost the same (64.9% and 61.3%). Lake Ontario has the largest STD compared to its mean, while Lake Erie has the smallest STD. The statistics for each lake reflects the effects of geographic location, depth (i.e., water heat storage), and size on the ice conditions over the lakes.

[13] The long-term mean (1963–2010) AMIC for the whole Great Lakes is 54.5%, and the standard deviation is 20.9%. In this analysis, winters with normalized AMIC greater than or equal to 0.7 ($\geq$69.2%) were identified as maximal ice cover winters, and winters with normalized AMIC less than or equal to -0.7 ($\leq$39.8%) were identified as minimal ice cover winters. The normalized AMIC is defined as the difference between the maximum ice concentration and its climatology (mean) divided by its standard deviation. The AMIC of the whole Great Lakes has a significant negative correlation (-0.87) with the Great Lakes area averaged winter surface air temperature (SAT) (Figure 3a) during the period 1963–2010, indicating that the interannual variability of Great ice cover is mainly controlled by the SAT.

2.2. NCEP/NCAR Reanalysis

[14] We used monthly National Center of Environment Prediction/National Centers of Atmospheric Research (NCEP) reanalysis data [*Kalnay et al.*, 1996] to investigate the relationship between Great Lakes ice and atmosphere circulation anomalies. The data are available from 1948 to present. The resolution is 2.5×2.5 degree. The climatology of the period 1948–2007 was calculated and subtracted from the individual months to obtain the monthly anomalies. Average (December–January–February, DJF) anomalies were calculated for each winter. In this study, SAT, surface winds, and 700 hPa geopotential heights were used.
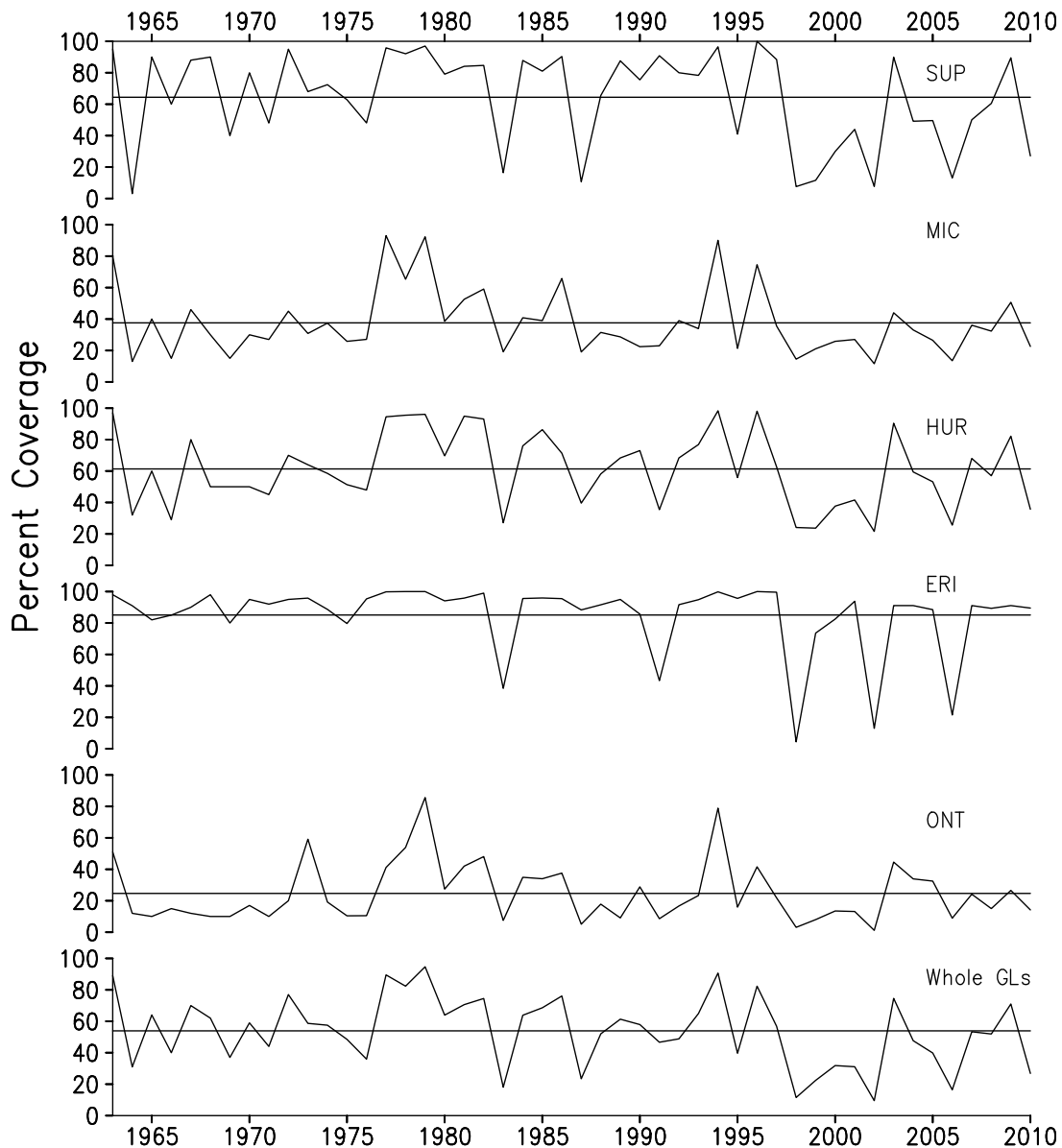
Figure 2. AMIC of all five lakes and the whole Great Lakes for the period 1963–2010.

2.3. Climate Indices

[15] The Nino3.4 Sea Surface Temperature (SST) anomaly index (Figure 3b) was used as a marker of ENSO variability to identify the warm and cold episodes during 1950–2010 based on a threshold of ±0.5°C. Cold and warm episodes are defined as those periods for which the threshold is met for a minimum of five consecutive overlapping seasons such as November–December–January (NDJ), December–January–February (DJF), January–February–March (JFM), etc. Otherwise, the winter is defined as ENSO-neutral. The index is defined as the 3 month running mean of ERSST.v3 (Extended Reconstructed Sea Surface Temperature Version 3) SST anomalies in the Niño 3.4 region (5°N–5°S, 120°–170°W; obtained from NOAA/CPC (Climate Prediction Center) http://www.cpc.noaa.gov/products/analysismonitoring/ensostuff/ensoyears.shtml). The strong warm (cold) winters are defined as the DJF periods

when the mean index exceeds 1.0 (−1.0) °C, and weak warm (cold) winters are defined as the DJF periods when the mean index greater than 0.5 (−0.5) °C, but less than 1.0 (−1.0) °C.

[16] The monthly NAO index from 1963 to 2010 was obtained from the Climatic Research Unit, UK (http://www.cru.uea.ac.uk/cru/data/NAO.htm) (Figure 3b). The NAO is defined as the normalized pressure difference between a

Table 1. Long-Term Mean and Standard Deviation of AMIC of Each Great Lake for the Period 1963–2010[a]

	Superior	Michigan	Huron	Erie	Ontario	Great Lakes
Mean (%)	64.4	37.6	61.3	85.1	24.7	54.5
SD (%)	29.4	20.9	23.0	22.1	18.8	20.9
SD/mean	0.46	0.55	0.38	0.26	0.76	0.38

[a]SD, standard deviation.
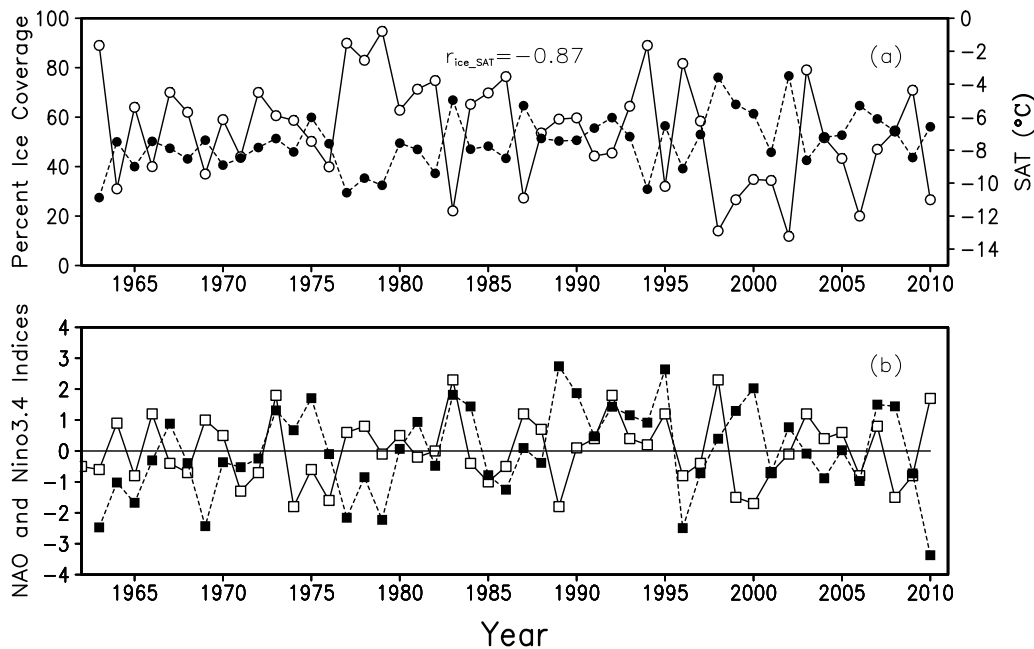
Figure 3. Time series of 1963–2010 (a) Great Lakes AMIC (solid) and Great Lakes basin averaged winter SAT (dashed) and (b) winter Nino3.4 (solid, in °C) and NAO (dashed, normalized) indices. Zero-lag correlations are calculated: r(ice, SAT) = −0.87, r(ice, Nino3.4) = −0.22, r(ice, NAO) = 0.27.

station on the Azores and one on Iceland. A winter is defined as a positive (negative) phase when the DJF mean index exceeds +0.5 (−0.5) standard deviation, otherwise a winter is defined as NAO-neutral.

2.4. Methods

[17] The main methods used in this study are correlation analysis (Pearson Correlation), multilinear regression, and composite analysis. Composite analysis is a common way to present the responses associated with a certain climate event such as ENSO and NAO by averaging the data over the years when the event occurred. To account for the small samples available in this study, the Student's t distribution was used to determine the statistical significance between means of two samples. Comparing the differences between two means using the Student's t test requires two independent samples of sizes n_1 and n_2, which possess means and standard deviations given by $\bar{x}_1$ and $\bar{x}_2$ and S_1 and S_2, respectively. Our null hypothesis, H_0, is that the two samples

are statistically indistinguishable from each other. To test H_0, we use the t score given by *Freund and Simon* [1992]

$$t = \frac{\bar{x}_1 - \bar{x}_2}{\sqrt{\frac{(n_1 - 1)s_1^2 + (n_2 - 1)s_2^2}{n_1 + n_2 - 2} \cdot \left(\frac{1}{n_1} + \frac{1}{n_2}\right)}}, \quad (1)$$

which is the value of a random variable having the t distribution with $n_1 + n_2 - 2$ degrees of freedom. The null hypothesis is rejected if the two-tailed t score exceeds the 90% confidence interval.

[18] Composite maps of winter mean anomalies associated with ENSO events over North America are obtained by subtracting El Niño (La Niña) seasonal means from the neutral ENSO seasonal mean at every grid. The t value of the difference between El Niño (La Niña) and ENSO-neutral was computed and superimposed in the composite map when the t value exceeds 10% and 5% significance levels. It is the same for NAO.

Table 2. Classification of Winters Based on Phases of ENSO and NAO[a]

	+NAO	−NAO	NAO-Neutral
El Niño	**1973**,[b,c] *1983*,[b,c] 1992,[b,c] *1995*,[b,c] 2007[c] (41.4) (state 1)	*1964*,[c] 1969,[b,c] **1977**,[c] **1978**,[c] 2010[b,c] (53.7) (state 3)	*1966*,[b] **1970**, *1987*,[b] 1988, *1998*,[b] ***2003***,[b] 2005
La Niña	**1974**,[b] 1975,[c] **1989**,[b,c] *1999*,[b,c] 2000,[b,c] 2008[b,c] (44.2) (state 2)	*1963*,[c] 1965,[c] 1971,[b] **1985** **1996**,[c] *2001* (62.4) (state 4)	**1968**, *1972*, *1976*[b]
ENSO-Neutral	*1967*, *1981*, **1984**,[c] **1990**,[c] **1993**,[c] *1994*, 2002	*1979*,[c] **1986**,[c] **1997**, 2004, 2006, ***2009***	1980, ***1982***, 1991

[a]The numbers in parentheses are the composite maximum ice concentration. Bold font indicates higher ice cover, bold italic indicates maximal ice cover, and italic font indicates minimal ice cover. Four major climate states are defined with the combined NAO and Niño3.4 indices.
[b]Strong El Niño/La Niña.
[c]Strong +/−NAO.

Table 3. Correlation Coefficients Between AMIC of Each Lake and Climatic Indices[a]

	Superior	Michigan	Huron	Erie	Ontario	Great Lakes
Nino3.4	−0.22	−0.14	−0.12	−0.21	0.074	−0.22
Nino3.4^2	**−0.47**	**−0.37**	**−0.43**	**−0.34**	**−0.34**	**−0.48**
NAO	−0.16	**−0.37**	−0.17	−0.15	−0.24	**0.27**
NAO^2	−0.02	0.14	0.098	0.13	0.067	0.1

[a]Bold font indicates that the correlations are significant at the 95% level.

3. Responses of Great Lakes Ice to NAO and ENSO

[19] From 1963 to 2010, there were a total of 14 maximal (≥69.2%) ice cover events on the Great Lakes during the winters of 1963, 1967, 1972, 1977, 1978, 1979, 1981, 1982, 1985, 1986, 1994, 1996, 2003, and 2009. There were a total of 15 minimal (≤39.8%) ice cover events during the winters of 1964, 1966, 1969, 1975, 1976, 1983, 1987, 1995, 1998, 1999, 2000, 2001, 2002, 2006, and 2010. Eight of 14 (∼57%) maximal ice winters coincided with −NAO events (see the years with bold italics in the third column of Table 2), and 8 of 15 (∼53%) minimal ice winters coincided with El Niño events (see the years in italic in the second row of Table 2). These imply that both NAO and ENSO have impacts on Great Lakes ice cover, and none of them dominates over the Great Lakes region. Table 3 lists the correlations between AMIC for each lake and the whole Great Lakes and NAO index and Nino3.4 index. None of the five lakes has significant correlation with Nino3.4 index. Lake Superior has the largest correlation, and Lake Ontario has the smallest correlation with Nino3.4. Lake Michigan has a significant correlation with NAO (−0.37). The Great Lakes as a whole has a significant correlation with NAO (0.27).

3.1. Great Lakes Ice Cover and NAO

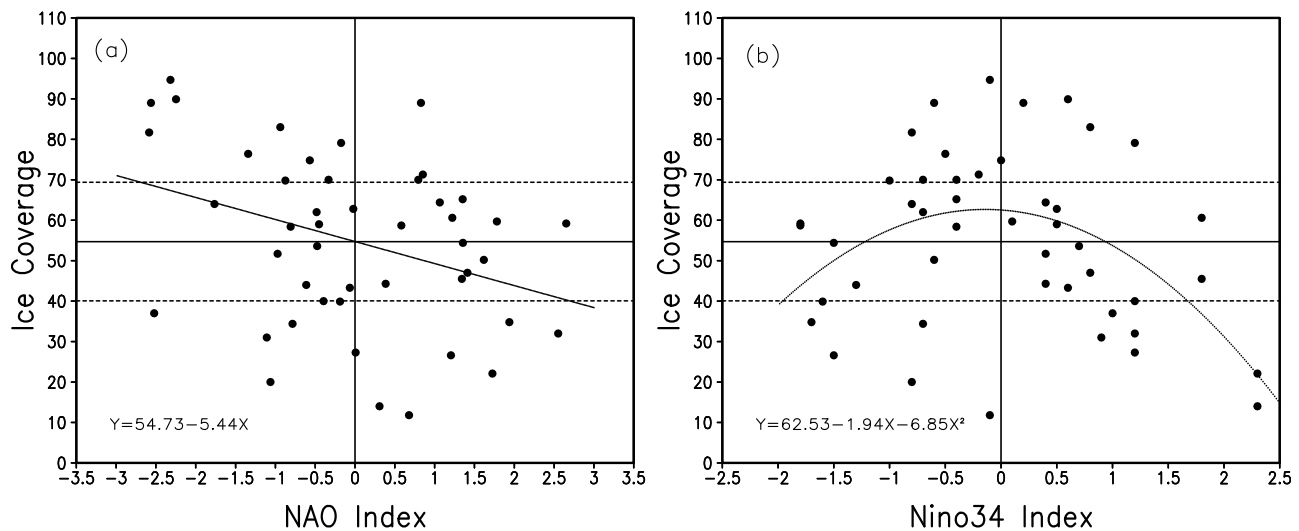[20] Figure 4 shows scatterplots between ice coverage and the NAO index (Figure 4a), and the Nino3.4 index

Table 4. Statistical Chi-Square Test of Relationship Between the NAO/ENSO and Lake Ice Cover[a]

	Above Normal Ice Cover	Below Normal Ice Cover
	Chi-Square Test: 0.45	
+NAO	1967, 1973, 1974, 1981, 1984, 1989, 1990, 1993, 1994 (9)	1975, 1983, 1992, 1995, 1999, 2000, 2002, 2007, 2008 (9)
−NAO	1963, 1965, 1977, 1978, 1979, 1982, 1985, 1986, 1996, 1997 (10)	1964, 1969, 1971, 2001, 2004, 2006, 2010 (7)
	Chi-Square Test: 2.43	
El Niño	1970, 1973, 1977, 1978, 2003 (5)	1964, 1966, 1969, 1983, 1987, 1988, 1992, 1995, 1998, 2005, 2007, 2010 (12)
La Niña	1963, 1965, 1968, 1972, 1974, 1985, 1989, 1996 (8)	1971, 1975, 1976, 1999, 2000, 2001, 2008 (7)

[a]The NAO indices are greater than ±0.5, and Nino3.4 indices are greater than ±0.5°C. The 95% and 90% significance chi-square thresholds are 3.84 and 2.71, respectively.

(Figure 4b). The relationship between NAO and Great Lakes ice cover is basically linear, with the correlation coefficient being 0.27, implying that the ice cover tends to be lower (higher) than normal during positive (negative) NAO. To confirm the linearity relationship, we also calculated the correlation between ice cover and square of NAO index, which is only 0.10 with no significance even at the 90% significance level.

[21] During the period 1963–2010, there were 17 negative NAO and 18 positive NAO events. Among them, there are 13 (9) strong positive (negative) NAO events. Ten of 17 negative NAO winters had above-average ice cover, while 5 negative NAO winters had remarkably low ice cover; 2 (1964 and 1969) during El Niño and 2 (1971 and 2001) during La Niña events at the same time. There were 18 positive NAO events of which 9 were associated with below-average ice cover (5 were minimal ice cover). Winters of

Figure 4. The plane scatterplots between ice coverage and (a) the NAO index and (b) the Nino3.4 index for the period 1963–2010. The regression curves are also calculated using the least square fit. The climatological, maximal, and minimal ice concentrations are 54.5%, 69.2%, and 39.8%, respectively. Note that −0.5 < index < 0.5 is a neutral state, 0.5 < |index| < 1.0 is a weak event, and 1.0 < |index| is a strong event.

(a) +NAO

(b) −NAO
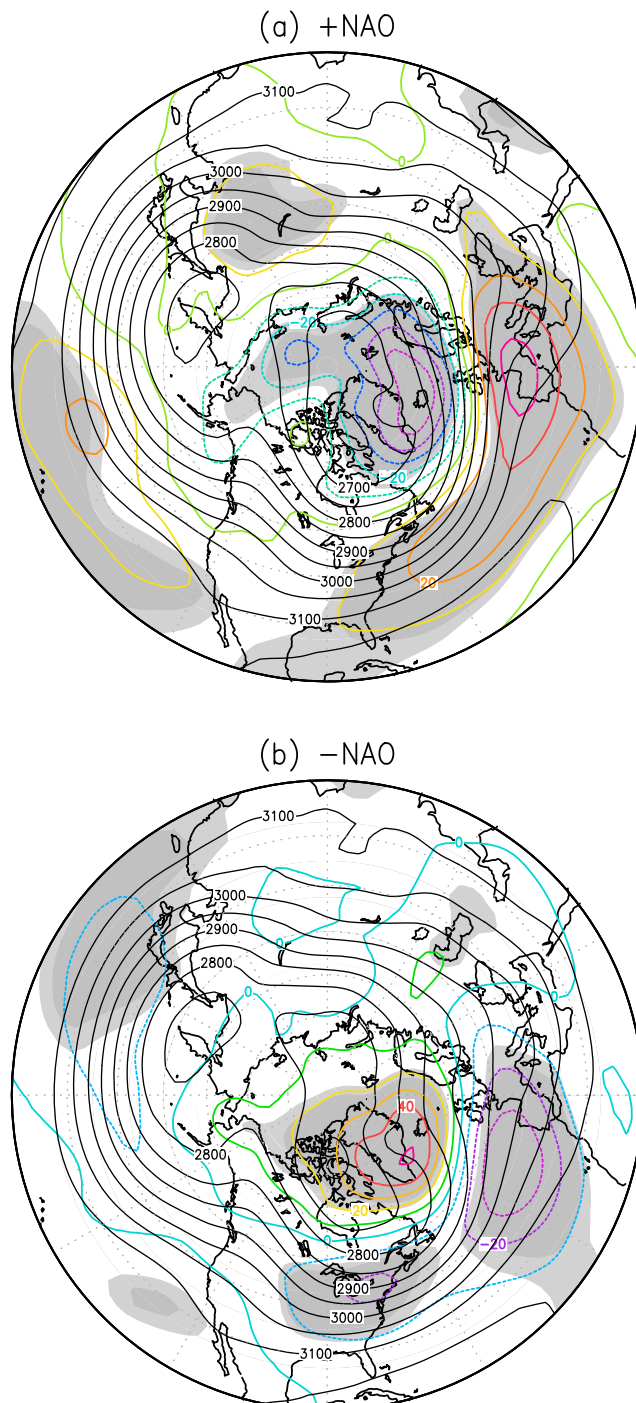
Figure 5. Composite maps of mean winter 700 hPa geopotential height (in black solid line) and anomalies (in color) (relative to NAO-neutral mean) for winters of (a) positive and (b) negative NAO during 1963–2010. The intervals for the means and anomalies are 50 and 10 m, respectively. The gray and dark gray shaded regions indicate the 95% and 99% significance level, respectively.

1967, 1981, and 1994 had maximal ice cover (see Tables 2 and 4).

[22] To examine the atmospheric conditions over the Great Lakes, composite maps of mean winter 700 hPa

height, surface winds, and SAT anomalies are constructed for positive and negative phases of NAO, respectively. The 700 hPa height anomaly field (Figure 5a) shows a positive AO-like structure: there is a significant negative anomaly in the Arctic including Iceland, and a positive anomaly in the midlatitude Atlantic Ocean [*Thompson and Wallace*, 1998; *Wang and Ikeda*, 2000; *Wang et al.*, 2005]. This strengthens the polar vortex and the westerly. An opposite scenario occurs during the −NAO composite anomaly map (Figure 5b), which leads to a weakening of the polar vortex and thus the westerly. The important feature of +NAO is that the midlatitude high anomaly advects warm air from the south by the southerly wind (Figure 6a) to the Great Lakes region. Thus, a warm winter can be expected during a +NAO event (Figure 6a). During the −NAO events, the westerly winds are weakened, a polar trough near the Great Lakes, and a ridge over the West Coast are developed (Figure 5b). This trough-ridge system promotes the penetration of Arctic air (northerly wind; see Figure 6b) into the Great Lakes region. Thus, a cold winter can be expected during a −NAO event (Figure 6b).

[23] Figure 6 presents the composite maps of SAT and wind anomaly associated with positive and negative NAO, respectively. During the positive phase of NAO, anomalous southerly winds dominate the Great Lakes, leading to insignificant warmer-than-normal temperatures ranging from 0.0 to 0.6°C (Figure 6a), although it is not over the 90% significance level. The mean ice coverage of all positive NAO winters is 51.8%, which is slightly lower than the long-term mean (54.5%). During the negative phase of NAO, anomalous northerly winds prevail over the upper lakes, and westerly winds prevail over the lower lakes. A strong cold SAT anomaly ranging from −0.9 to −1.8°C appeared in the Great Lakes region with the 95% significance level. The western lakes are colder than the eastern lakes (Figure 6b). The average ice coverage of negative NAO winters is 62.5%, which is higher than the long-term mean (54.5%). The mean ice coverage of strong positive and strong negative NAO events is 47.6% and 64%, respectively.

[24] The evidence shown in Figure 6 suggests that Great Lakes ice cover is influenced by NAO. The Great Lakes region tends to be colder (warmer) than normal and have higher (lower) ice cover during negative (positive) NAO. The negative NAO coincides with 8 out of 14 maximal ice events. However, most of the minimal ice cover (Figure 3a) did not occur during a positive NAO, but during strong El Niño events (Figure 3b). Furthermore, there are strong negative NAO winters that are not associated with maximum ice cover, such as the winters of 1964, 1969, and 2010, during which minimal ice cover occurred instead. The winters of 1964, 1969, and 2010 were during El Niño events. Apparently, in addition to NAO, ENSO is also an important factor in influencing Great Lakes ice conditions, which will be discussed in section 4.

[25] To provide statistics of individual climate patterns and lake ice cover, we conducted a simple statistical chi-square test of the statistical relationship between the NAO and lake ice cover (Table 4). There is no difference during the +NAO events, as there are 9 each above-normal and below-normal ice winters. During the −NAO events, there are 10 above-normal and 7 below-normal ice winters, which

(a) +NAO

(b) −NAO
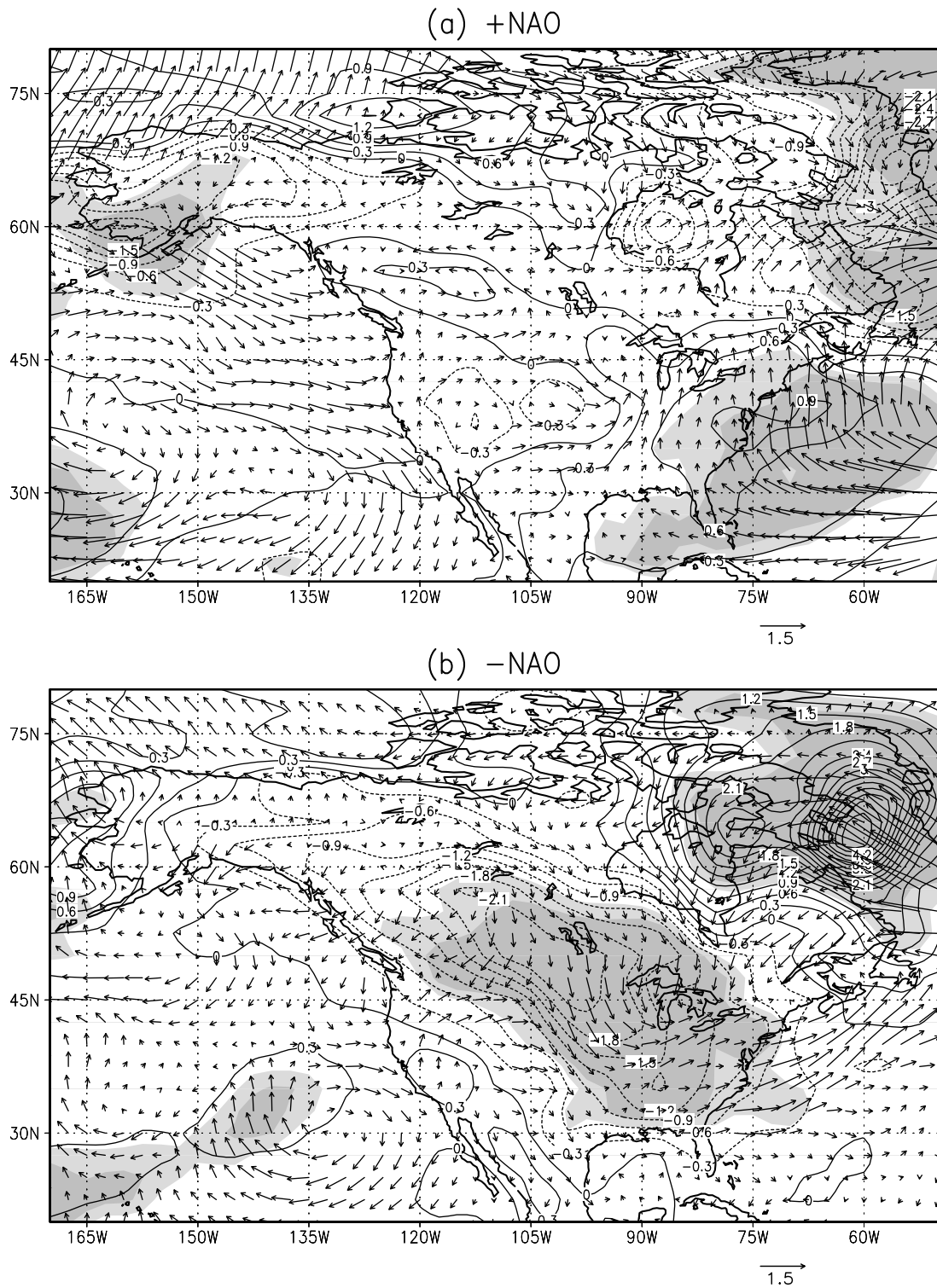
Figure 6. Composite maps of mean winter SAT and surface wind anomalies (relative to NAO-neutral mean) for winters of (a) positive and (b) negative NAO during 1963–2010. The SAT intervals are 0.3°C. Shaded areas are locally significant in SAT field at the 10% (lighter) and 5% (darker) levels relative to NAO neutral based on a two-tailed *t* test.

has no significant difference. Thus, the overall chi-square test is 0.45, far below the 95% (3.84) and at 90% (2.71) significance levels. This indicates that the predictability skill for lake ice using the sole NAO index is poor. The same conclusion can be drawn for the strong NAO (NAO index ≥ ±1) and strong ENSO events (Nino3.4 index ≥ ±1°C) (not shown).

3.2. Great Lakes Ice Cover and ENSO

[26] The nonlinear relationship between Nino3.4 and Great Lakes ice cover is clearly identified in Figure 4b. The higher-than-average points (ice cover) are likely to be confined between −1.0 and 1.0 (weak or neutral ENSO episodes), while the lower-than-average dots are more scattered and tend to occur during strong El Niño or strong La Niña events, indicating that most of the maximal ice cover occurred during weak or neutral ENSO episodes, and most of the minimal ice cover occurred during strong El Niño or strong La Niña events.

[27] Although the correlation between Nino3.4 index and ice coverage is not significant (−0.22) from zero, the correlation coefficients between the quadratic Nino3.4 index and AMIC for each lake and the whole Great Lakes turn out to be significant at the 95% confidence level (Table 3). The upper lakes have a closer relationship with Nino3.4^2 than the lower lakes. Lake Superior has the largest and Lakes Erie and Ontario have the smallest correlations with Nino3.4^2 (Table 3). The nonlinear effects of ENSO on Great Lakes ice cover are important in addition to NAO effects.

[28] During the period 1963 to 2010, there were 17 El Niño events: 1964, 1966, 1969, 1970, 1973, 1977, 1978, 1983, 1987, 1988, 1992, 1995, 1998, 2003, 2005, 2007, and 2010; and 15 La Niña events: 1963, 1965, 1968, 1971, 1972, 1974, 1975, 1976, 1985, 1989, 1996, 1999, 2000, 2001, and 2008. The mean ice coverage of all El Niño and La Niña winters is 47.8% and 53.5%, respectively. The former is lower than the long-term mean (54.5%), while the latter is close to the long-term mean. Twelve of 17 El Niño winters had lower ice cover (Table 4); among which 7 out of 10 strong El Niño winters (Nino3.4 ≥ 1.0) had minimal ice cover. Five of 17 El Niño winters had high ice cover (1970, 1973, 1977, 1978, and 2003) (Table 4), among which 3 winters (1977, 1978, and 2003) had maximal ice cover. The winters of 1977 and 1978 were also during strong negative NAO events.

[29] The impact of La Niña events on Great Lakes ice cover is complicated. *Assel and Rodionov* [1998] claimed that association between La Niña events and above-average ice cover on the Great Lakes basin is much weaker and less stable than El Niño events. It is true that most of the maximal ice cover seasons are often associated with negative NAO, but not with La Niña events. There were 15 La Niña events that occurred during the study period. Eight winters had higher and seven had lower ice cover (Table 4). Four minimal ice cover events occurred in La Niña events (1976, 1999, 2000, and 2001; see the years with italic in the third row of Table 2). Five of seven strong La Niña events were associated with low ice cover (see the years with b footnote in the third row of Table 2). Six of eight weak La Niña events were associated with high ice cover (see the years with bold and without the b footnote in the third row of

Table 2). The evidence suggests that the influence of La Niña on Great Lakes ice cover is intensity-dependent.

[30] Figures 7a, 7b, 7c, and 7d present composite wintertime (DJF) 700 hPa heights and anomalies for the ten strong (seven weak) El Niño events and the seven strong (eight weak) La Niña events, respectively. The 700 hPa height anomalies for strong El Niño events (Figure 7a) show a clear negative TNH signature with negative anomalies over the Gulf of Alaska and southeastern United States, and positive anomalies over Hudson Bay and the Great Lakes region, while the map for weak El Niño events show a typical positive PNA pattern with negative anomalies over the North Pacific Ocean and southeastern United States, and positive anomalies over Alberta (Figure 7b). The 700 hPa height anomalies for strong and weak La Niña events all resemble a negative PNA pattern (Figures 7c and 7d). It is evident that the Great Lakes are positioned in between the action centers of PNA pattern during La Niña and weak El Niño events, while they are covered by the positive center of TNH pattern during strong El Niño events. It is expected that the impacts of La Niña and weak El Niño events on Great Lakes ice cover will be less remarkable than the strong El Niño events. The action centers of the TNH associated with strong warm events are shifted eastward with respect to those of a typical PNA pattern associated with cold events. *Hoerling et al.* [1997, 2001] attribute the phase shift in the teleconnection patterns to the phase shift between El Niño and La Niña convection (rainfall) anomalies. Due to the zonal asymmetries of the climatological SSTs in the tropical Pacific Ocean with the warm pool in the west and the cold tongue in the east, even small SST anomalies can excite large rainfall anomalies on the periphery of the west Pacific warm pool region, whereas positive anomalies of appreciable amplitude are required to induce convection within the east equatorial Pacific cold tongue, because little convective activity takes place over SST values of colder than 27°C. On the other hand, negative SST anomalies in the cold tongue region have no further effect on the normally dry conditions. Thus, the analysis of OLR (outgoing long-wave radiation, a proxy of rainfall in the tropical region) data suggests that maximum positive rainfall anomalies are located east of the dateline during an El Niño event, but slightly west of the dateline during a La Niña event.

[31] During strong El Niño events, the TNH pattern reflects that strong El Niño events are usually associated with a deeper-than-normal trough over the Gulf of Alaska, a weaker-than-normal ridge over the west coast, and a weaker-than-normal Hudson Bay trough over eastern Canada. These upper circulation anomalies prevent a cold Arctic air mass from intruding from the north to the Great Lakes region, allowing the warm Pacific air to flow to the high latitudes, and leading to a warmer winter in the northern U.S. including the Great Lakes region. Anomalous easterly and northeasterly winds prevail over the Great Lakes region, weakening the climatological westerly winds. The maximum warm temperature anomaly during strong El Niño events is located over south central Canada with the Great Lakes region at its southeast, close to the warming center. The warming over the Great Lakes is significant (0.6–1.8°C). The warming decreases from northwest to southeast with the greatest warming over Lake Superior and the smallest warming over Lakes Erie and Ontario (Figure 8a). The remarkable warming
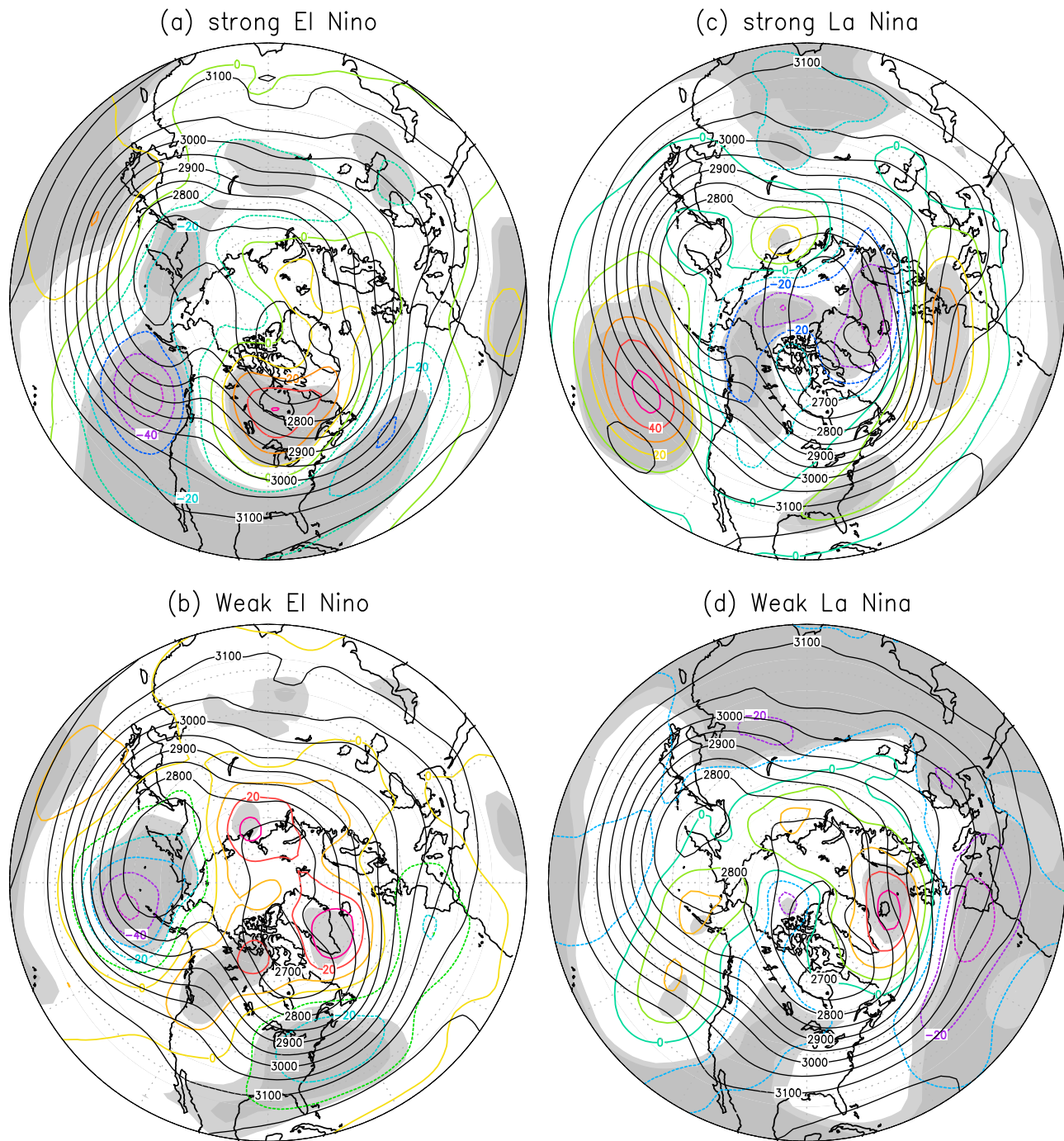
Figure 7. Composite maps of mean winter 700 hPa height (in black solid lines) and anomalies (in color) for winters of (a) strong El Niño, (b) weak El Niño, (c) strong La Niña, and (d) weak La Niña. The intervals for the means and anomalies are 50 and 10 m, respectively. The gray and dark gray shaded regions indicate the 95% and 99% significance level, respectively.

and weakened winds (reduced turbulence sensible and latent heat loss) are all favorable for less ice formation.

[32] During weak El Niño events, the positive PNA type distribution of 700 hPa anomalies produces a stronger-than-normal trough along the east coast and a stronger-than-normal ridge over the west coast of North America. The amplified ridge-trough system resulted in a meridional flow regime with increased advection of cold polar air masses into the eastern portion of North America. Anomalous northwesterly winds (Figure 8b) prevail over the Great Lakes region. The SAT anomalies indicate significant warming along the west coast of North America, west and central Canada, and cooling in the southern U.S. and the Gulf of Mexico. The Great Lakes are positioned right in
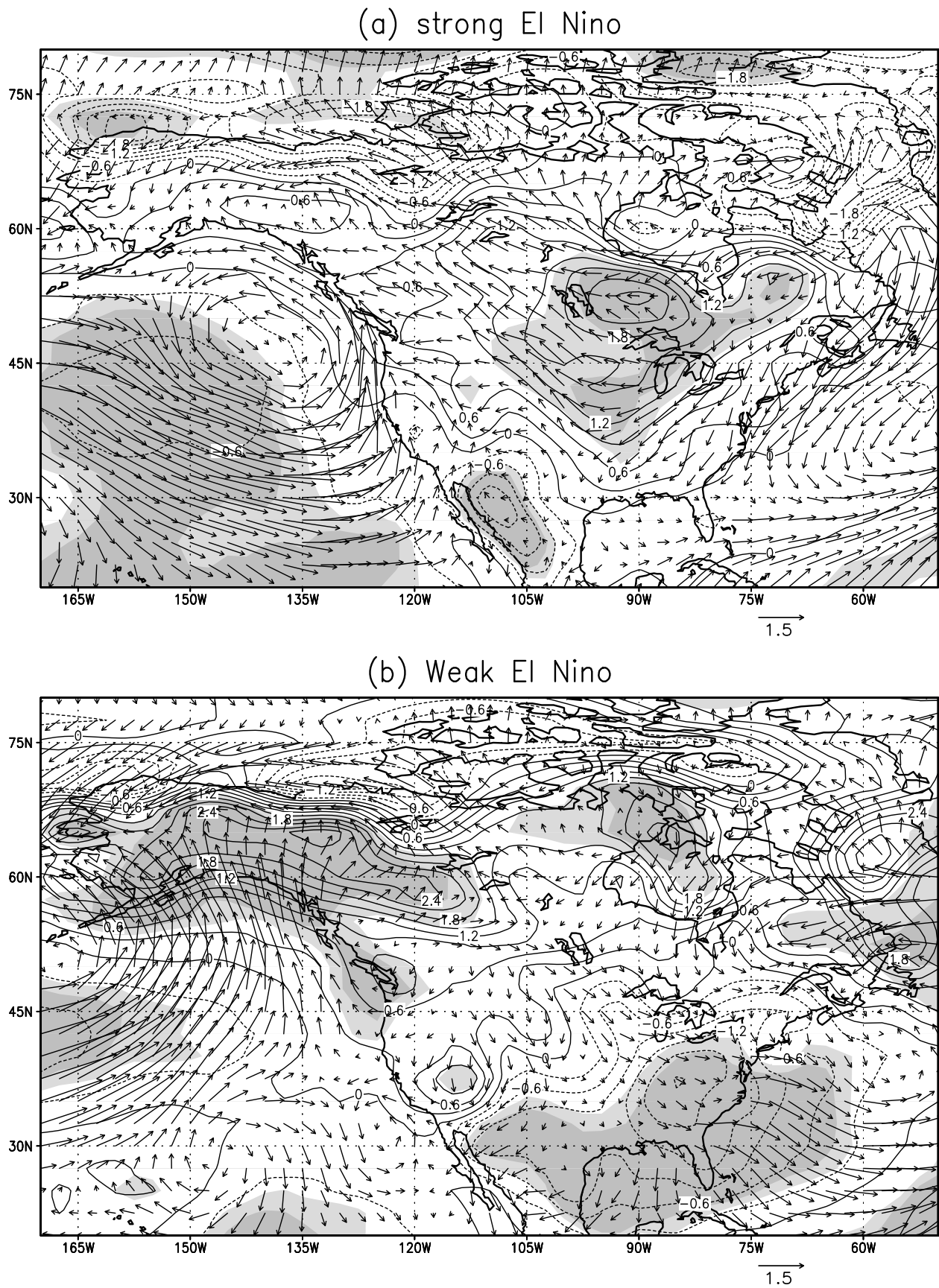
(a) strong El Nino
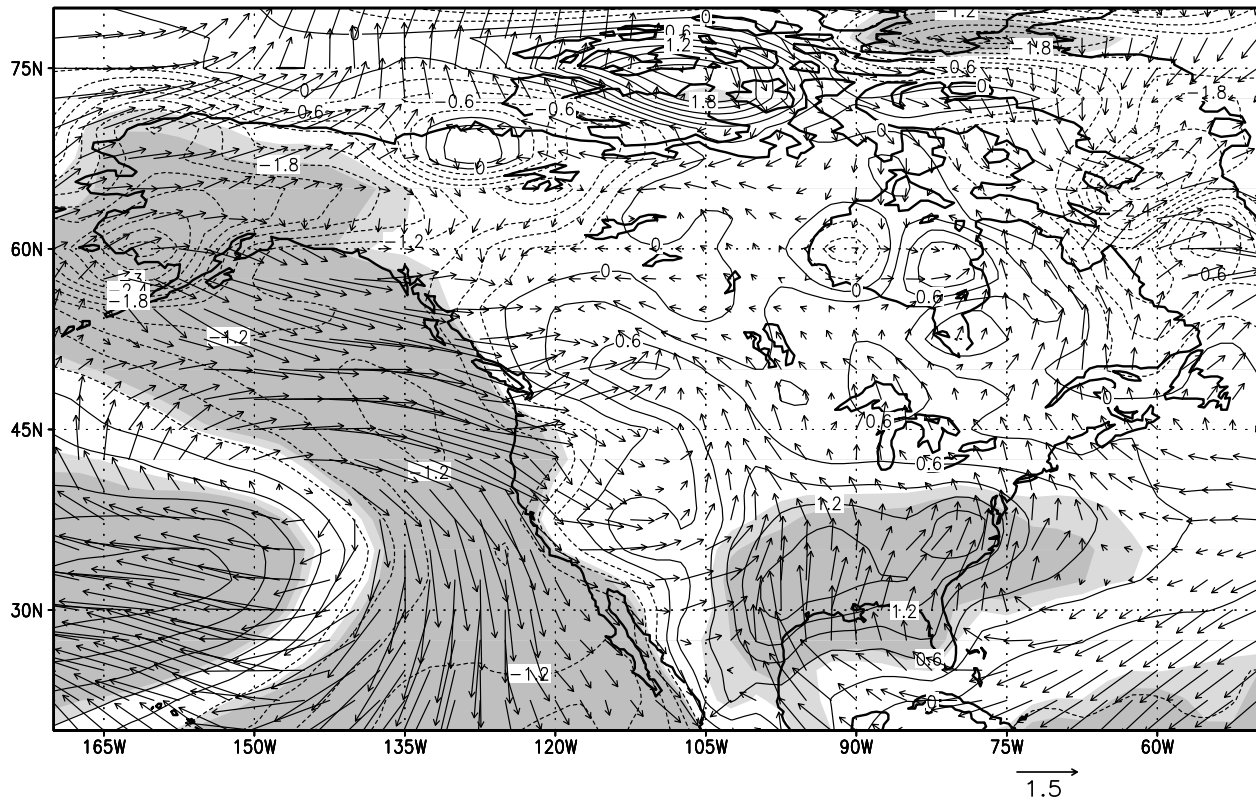

(b) Weak El Nino

Figure 8. (a–d) Same as Figure 7 but for SAT and surface wind anomalies. The intervals and shading schemes are the same as Figure 6.

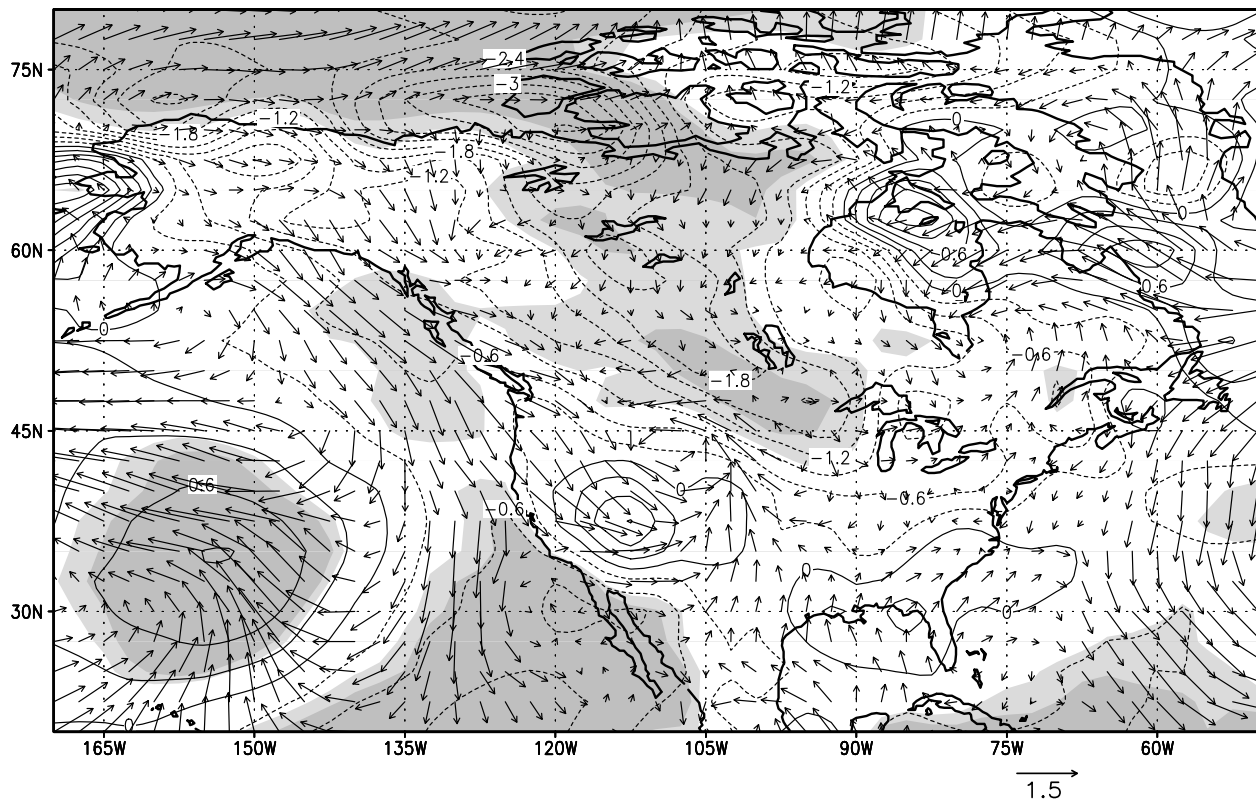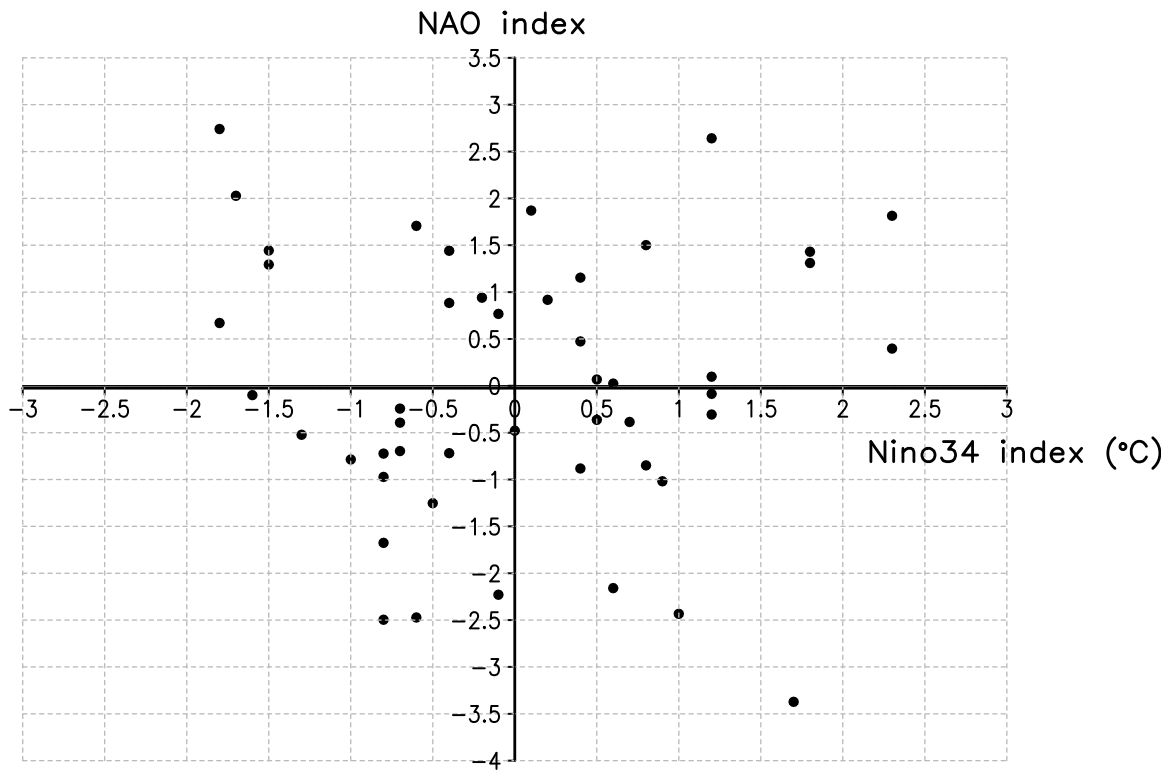## (c) strong La Nina

(d) Weak La Nina

Figure 8. (continued)

Figure 9. The plane scatterplot between NAO and Nino3.4 index for the period 1963–2010.

between the warming and cooling centers with insignificant cooling (0.3–1.2°C) over the lower lakes and a slight warming over Lake Superior, suggesting the weak El Niño has insignificant impacts on Great Lakes ice cover.

[33] During strong La Niña events, associated with the negative PNA pattern (Figure 7c), the SAT anomaly shows significant below-average temperatures over Alaska and the west coast of North America, and above-average temperatures across the south central and southeastern United States (Figure 8c). The Great Lakes are positioned on the left side of the positive center over the southeastern tier of the U.S., with the zero isoline across Lakes Michigan and Huron (Figure 7c). The anomalous southerly or southwesterly flow on the left side of the southeastern positive center brings warm air from the south, leading to warmer-than-normal temperatures (about 0.6°C) (Figure 8c) and lower ice cover (Figure 4b). However, as the Great Lakes are positioned on the edge of the action center, the response of SAT to strong La Niña events is not as significant as strong El Niño events. Although the composite 700 hPa height anomaly for strong and weak La Niña events all resembles a negative PNA, the difference is obvious (Figures 7c and 7d). The negative PNA pattern for the strong La Niña events is stronger than the weak ones. For example, the positive anomalies over the southeastern tip of the U.S. are statistically significant during strong La Niña events relative to that during weak ones. During weak La Niña events, anomalous westerly winds prevail over the Great Lakes, leading to colder-than-normal temperature (−1.2 to 0°C) (Figure 8d), and thus leading to higher ice cover (Figure 4b).

[34] The above evidence suggests that the Great Lakes tend to be warmer than normal and thus, have lower ice cover during El Niño events, especially during strong El Niño events. During La Niña events, although ice conditions on the Great Lakes are difficult to project, the Great Lakes tend to be warmer (colder) than normal during strong (weak) La Niña events, which is similar to El Niño events. This nonlinear, asymmetric response of Great Lakes ice to ENSO is due to the phase shift of the teleconnection patterns during the different phases of ENSO, which is consistent with the recent finding that impacts of ENSO on North American surface temperature is nonlinear and asymmetric [*Livezey et al.*, 1997; *Hoerling et al.*, 1997, 2001; *Wu et al.*, 2005].

[35] We further conducted the chi-square test of the relationship between the Nino3.4 index and anomalous ice cover (Table 4). During the El Niño events, there are 5 above-normal and 12 below-normal ice winters, which has a significant difference. However, during La Niña events, there are 8 above-normal and 7 below-normal ice winters, which has no significant difference. This further indicates the asymmetric response of lake ice to El Niño and La Niña events. The overall chi-square threshold is 2.43, below the 95% significance level (3.84) but close to the 90% significance level (2.71).

4. Combined Effects and Interference of NAO and ENSO

[36] Because both ENSO and NAO impact the Great Lakes region, the combination and interference of these two factors must be considered in the investigation of the relationship between lake ice and ENSO or NAO. The most important is that a −NAO and a strong El Niño can explain most of the maximal and minimal events, respectively. This

implies that the two effects should be taken into account when predicting Great Lakes ice conditions. As mentioned above, most of the El Niño events were associated with lower-than-normal ice cover. Coinciding with a positive NAO or NAO-neutral can reinforce this relationship. However, when a winter happens to be in a state of −NAO/El Niño, ice conditions on the Great Lakes depend on these two competing forcings. For example, winter 1969 was in a strong El Niño and a negative NAO, and minimal ice cover occurred. Winters of 1977 and 1978 were in a weak El Niño and a negative NAO and had high ice cover (note that 1977 and 1978 had maximal ice cover) since the −NAO-derived cooling surpassed the El Niño-derived warming.

[37] Figure 9 and Table 2 show that many −NAO events coincide with weak El Niño or weak La Niña events, while many +NAO events coincide with strong El Niño or strong La Niña events. The stronger −NAO impacts surpass the weak El Niño or weak La Niña impacts and produce heavy ice cover, which introduces an arc-shaped curve in the upper part (Figure 4b); this is why most of the maximal ice cover occur during a neutral or weak ENSO. The simultaneous +NAO and La Niña events produce low ice cover, which further enhances the asymmetric response of the Great Lakes winter climate (and ice cover) to ENSO. The nonlinear response of Great Lakes winter climate (and ice cover) to ENSO is partly due to the interference or combined effects of these two forces.

[38] To demonstrate the combined effects of NAO and ENSO, the winters were classified into nine groups based on phases of ENSO and NAO (see Table 2). We mainly examined the four climate states: (1) +NAO/El Niño, (2) +NAO/La Niña, (3) −NAO/El Niño, and (4) −NAO/La Niña. In general, as discussed in section 3, the Great Lakes tend to be warmer than normal and have less ice cover during El Niño events or +NAO events, and are colder than normal during −NAO or La Niña events. Note that La Niña events have weaker impacts on lake ice than El Niño events (i.e., the asymmetric influence). Thus, when a winter falls into simultaneous +NAO and El Niño episodes (state 1), it is expected to be warmer and have less ice cover, since +NAO and El Niño have the same warming effect on the Great Lakes. When a winter falls into −NAO and La Niña events at the same time (state 4), it is expected to be colder and produce more ice cover. Furthermore, if a winter happens to be in the state of −NAO/El Niño (state 3) or +NAO/La Niña (state 2), the competition of the two opposite effects (NAO and ENSO) will complicate the relationship.

[39] During 1963–2010, five winters fall into state 1 (+NAO/El Niño; see Table 2). The average ice coverage for these winters is 41.4%, which is well below the long-term mean (54.5%), and is also lower than the mean ice cover of all El Niño winters (47.8%). The mean 700 hPa height anomalies (Figure 10a) of these five winters clearly indicates +NAO and El Niño signatures with low anomalies over the Arctic and North Pacific off the west coast of North America; high anomalies over the Great Lakes region, Western Europe, and the adjacent North Atlantic. At the surface (Figure 11a), anomalous easterlies prevail over the Great Lakes, which weakens the climatological westerly winds (not shown). Positive SAT anomalies over the Great Lakes ranged from 1.2 to 1.5°C (Figure 11a).

[40] Six winters fall into state 4 (−NAO/La Niña), and the mean ice cover is 62.4% (Table 2), which is larger than the long-term mean (54.5%) and all −NAO means (60.6%). All the winters except 2001 had above-average ice cover, and winters of 1985 (69.8%) and 1996 (81.7%) had severe ice cover. The composite map of 700 hPa height anomalies for these five winters (Figure 10d) shows positive anomalies are located over the Arctic, the west coast off western Canada, and Alaska. Anomalous northwesterly winds prevail over the Great Lakes, which enhances the climatological westerly and brings cold air from the northwest, leading to colder-than-normal temperatures in the Great Lakes (Figure 11d). Colder-than-normal temperatures appeared in almost all of North America with a center located to the northwest of the Great Lakes (Figure 11d). The SAT anomalies in the Great Lakes ranged from −0.6 to −1.2°C. The difference between the mean SAT for state 1 (+NAO/El Niño) and for state 4 (−NAO/La Niña) is significant over the Great Lakes area.

[41] Five winters fall into state 3 (−NAO/El Niño; Table 2). Their mean ice coverage is 53.7%, which is close to the long-term mean (54.5%), but lower than the all −NAO mean (60.6%) and larger than the all El Niño mean (47.8%). This indicates a competition of the effects of El Niño (warming) and −NAO (cooling). Although the competition, generally speaking, occurs in climate state 3, we can observe from Table 1 that there are both heavy ice winters (1970, 1977 and 1978) and light ice winters (1964 and 1969). This indicates that one climate pattern seems to dominate over the other. It is noted that even during −NAO events, the strong El Niño–derived warming in winters of 1964 and 1969 still surpassed the −NAO-derived cooling, leading to least ice cover. On the contrary, when weak El Niño events coincided with a negative phase of NAO, such as winters of 1970, 1977, and 1978, ice cover on the Great Lakes was above average. The evidence suggests that the Great Lakes area is a competing region for these two major forcings. When an El Niño event was strong, its warming could significantly influence the Great Lakes region and dominates the region over the influence of a negative phase of NAO (cooling). However, when El Niño events are weak, its influence cannot compete with the negative phase of NAO. Thus, when El Niño coincides with a negative phase of NAO, ice conditions on the Great Lakes depend on the strength between El Niño and −NAO.

[42] The composite 700 hPa height anomalies (Figure 10b) shows positive anomalies over an area north of 50°N; negative anomalies over the North Pacific, the Gulf of Mexico coast region, and the North Atlantic. Note that the Great Lakes are located close to the nodal (zero) line, indicating the unpredictability due to the fact that any displacement of these action centers can change the sign of the anomalies over the Great Lakes region. At the surface (Figure 11b), anomalous northerly winds prevail over the Great Lakes region. A SAT anomalies map (Figure 11b) shows remarkable warmer-than-normal temperatures in Alaska and Canada and colder-than-normal temperatures in the southeastern U.S. and over the Great Lakes. Although the cooling over the Lower Lakes is over 95% significance level, it is not significant over Lake Superior. Thus, the predictability skill for lake ice cover in climate state 3 is poor, indicating that case studies are
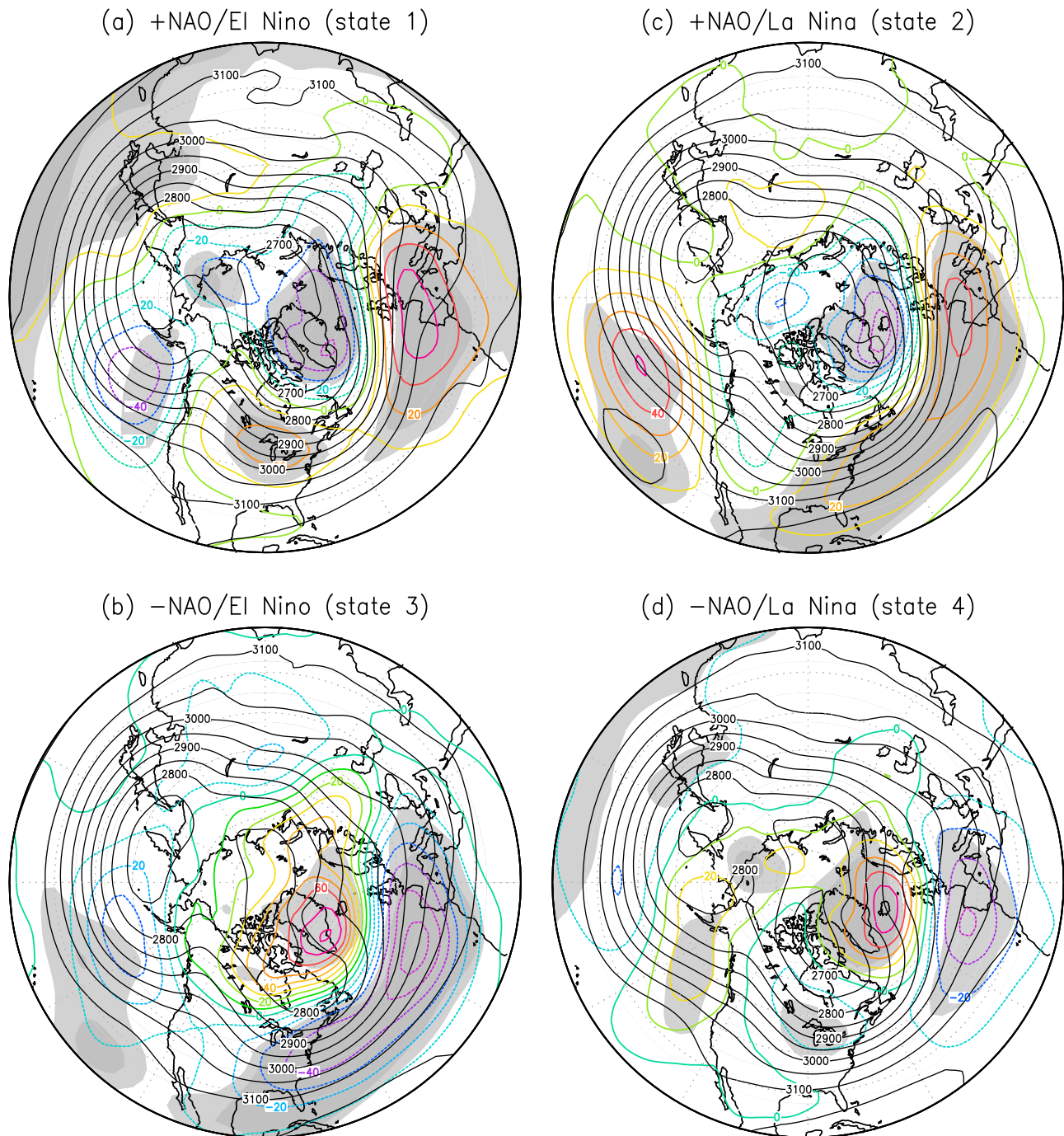
Figure 10. Composite maps of mean winter 700 hPa height (in black solid lines) and anomalies (in color) in North America for winters in states (a) 1, +NAO/El Niño; (b) 3, NAO/El Niño; (c) 2, +NAO/La Niña; and (d) 4, −NAO/La Niña. Shaded area indicates differences that are locally significant at the 5% level based on a two-tailed *t* test. The intervals for the means and anomalies are 50 and 10 m.

necessary for understanding the climate forcing on lake ice change.

[43] Six winters fall into state 2 (+NAO/La Niña; Table 2), and the average ice coverage is 44.2%, which is below the long-term mean (54.5%). The composite 700 hPa height anomalies (Figure 10c) show negative anomalies over an area poleward of 50°N and the Great Plains; positive

anomalies over the North Pacific and the area extending northeastward from Mexico to Western Europe across the North Atlantic. The Great Lakes are in between the positive and negative anomalies with a nodal line across the Lakes, indicating again the poor predictability skill, similar to state 3. At the surface (Figure 11c), southerly winds prevail leading to warmer-than-normal temperatures over the

(a) +NAO/El Nino (state 1)
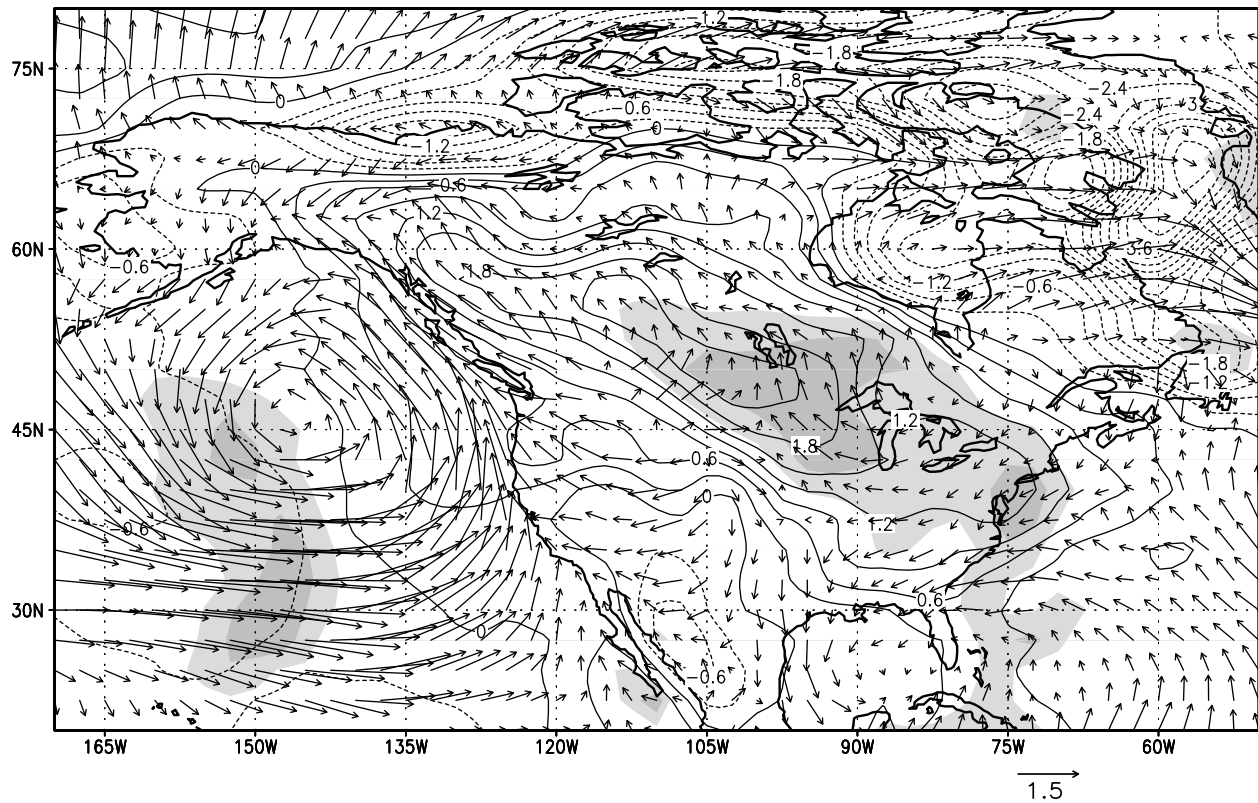
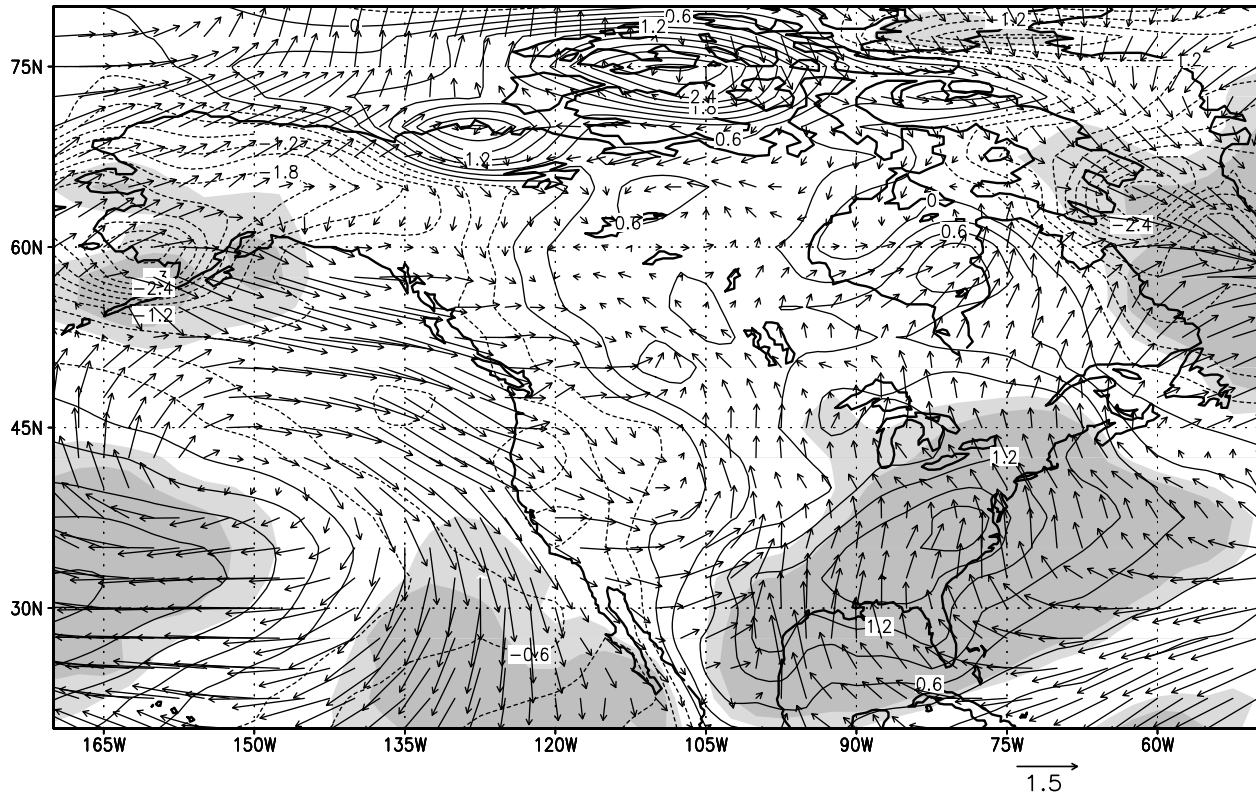## (b) −NAO/El Nino (state 3)
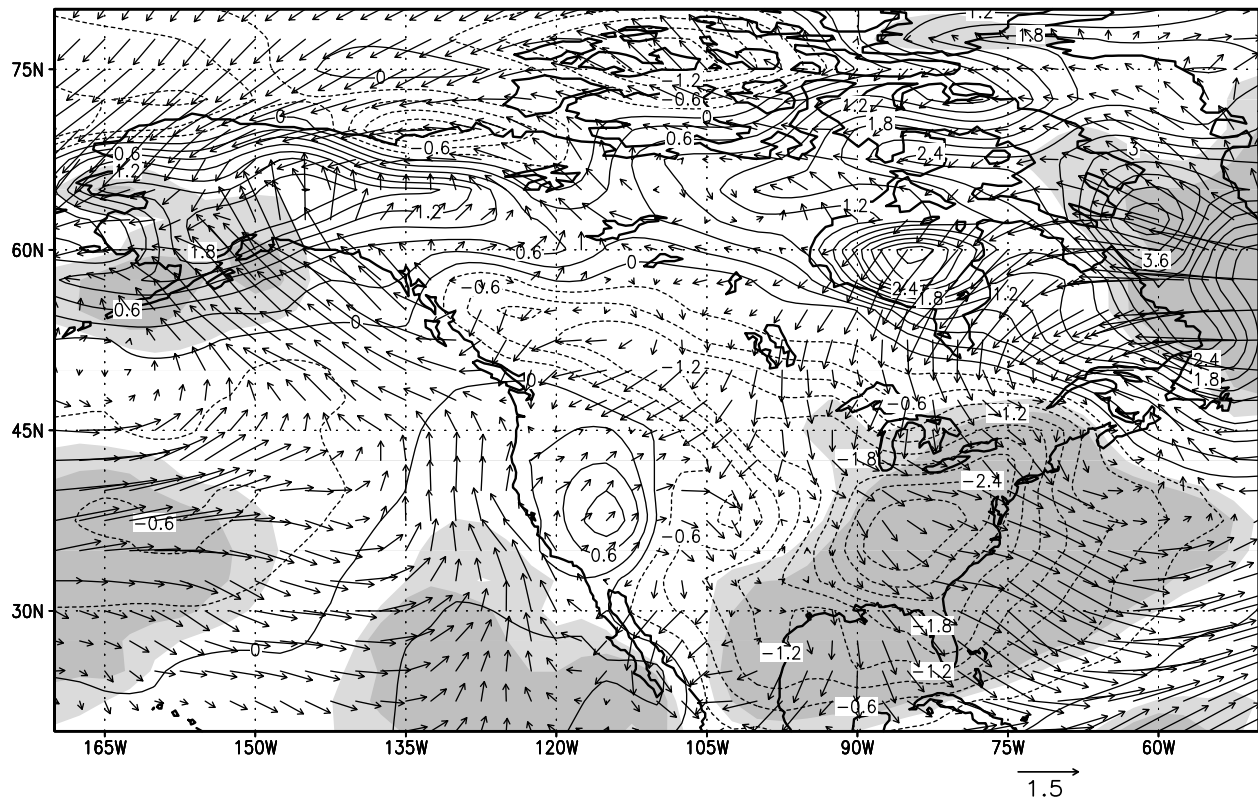
Figure 11. (a–d) Same as Figure 10 but for SAT (contour) and surface wind anomalies. The intervals of SAT anomalies are 0.3°C.

(c) +NAO/La Nina (state 2)
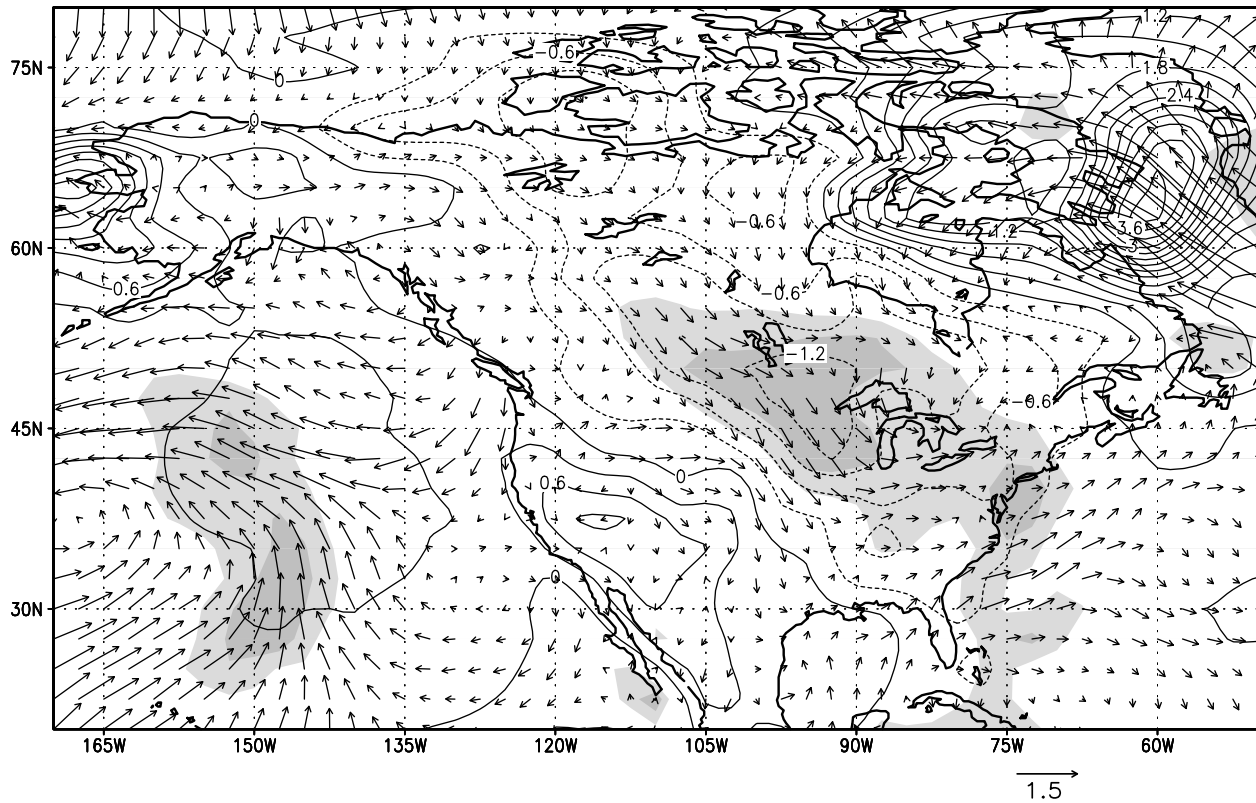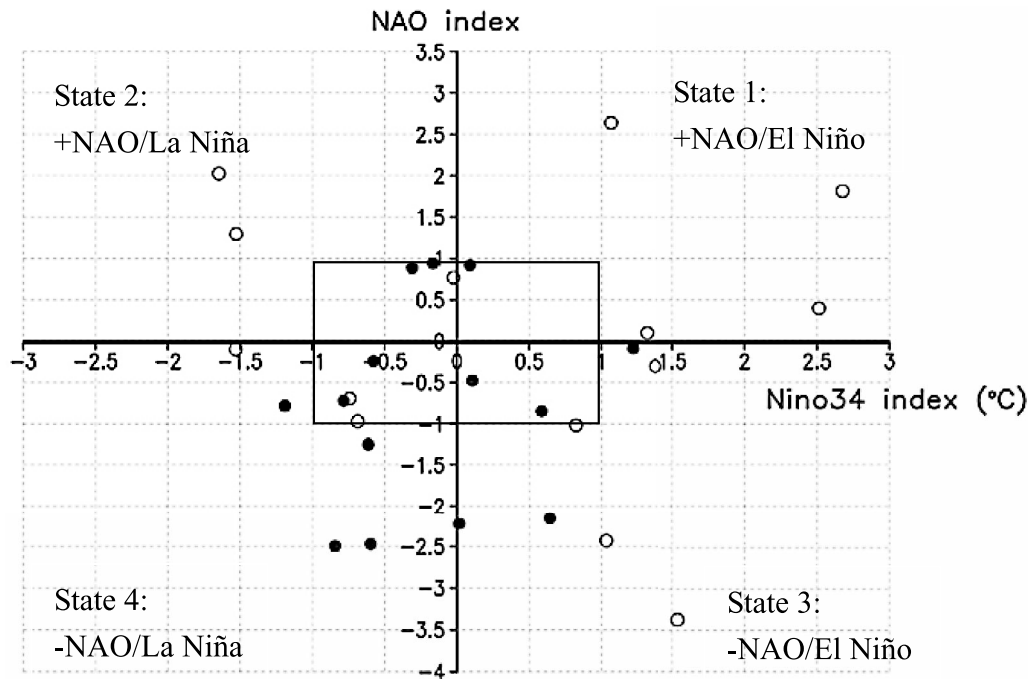
(d) −NAO/La Nina (state 4)

Figure 11. (continued)

Figure 12. The plane scatterplot of severe (solid) and mild (circle) winters with the Nino3.4 index as the *x* axis and the NAO index as the *y* axis.

Midwest and the eastern U.S., including the Great Lakes. The composite SAT anomalies in the Great Lakes range from 0.6 to 1.2°C (Figure 11c). As discussed in section 3, the SAT in the Great Lakes associated with La Niña events are slightly warmer than normal, which is not significant enough to produce abnormal ice cover. However, when coincided with +NAO, the above-average 700 hPa heights over the North Pacific and southeastern tier of the U.S. are enhanced. The enhanced pressure gradients in the Great Lakes region induce anomalous southerly winds, leading to warmer-than-normal temperatures in the Great Lakes.

[44] To clearly address the combined impacts of the NAO and ENSO on Great Lakes ice cover, we further constructed a scatterplot of maximal (solid circles) and minimal (open circles) ice cover on the Nino3.4-NAO index plane (Figure 12). In state 1, there are four minimal ice winters and one maximal ice winter (on the edge of the box). By contrast, in state 4, there are four maximal ice winters and one minimal ice winter (on the edge of the box), indicating these two states do provide liable predictability potential during both strong NAO and strong ENSO events. However, the competition can be seen in states 2 and 3. In state 2, there are two minimal ice winters and two maximal ice winters (on the edge of the box). In state 3, there are three maximal ice winters and four minimal ice winters.

5. Multiple-Variable Linear and Nonlinear Regression Models

[45] It must be pointed out that the combined NAO and ENSO cross-composite analyses as discussed in section 4 are based on limited samples in each climate state due to the limited length of the ice data records. However, the findings do shed light into the complexity of the nature in Great Lakes ice variability. Thus, a regression model can be developed based on the findings, as discussed in sections 3 and 4, to hindcast Great Lakes ice coverage. The model takes the following form

$$y = b_0 + \sum_i^n b_i x_i (n = 1, 2, \ldots N), \qquad (2)$$

where y is the normalized ice coverage, x_i is the predictor; b_0 and b_i are constants that are determined from observational data. Note that the normalized Nino3.4 and NAO indices are used in the regression models. The Nino3.4 index during 1963–2010 has a mean of 0.037°C and standard deviation of 1.076°C, and the NAO index has a mean of zero and standard deviation of 1.4. We used statistical software R to obtain the fitting models. All necessary model summaries and diagnostic information is listed in Table 5. For an overall assessment of the model, we often use the R^2 and a hypothesis test (the *F* test) to compare the fitted model and a model with no predictor variable. A *t* test is used to assess whether an individual predictor is necessary. Adjusted R^2 is defined by $R_{adj}^2 = 1 - \frac{n-1}{n-p}(1 - R^2)$, where n is the sample size, and p is the number of predictors. Adjusted R^2 is a statistic that may not increase if a predictor is added to a model; while R is always increased [*Qian*, 2009].

[46] We first tried a linear hindcast model with the Nino3.4 and NAO indices as predictors by using the method of least squares:

$$y = 5.78 \times 10^{-5} - 0.27 Nino3.4 - 0.23 NAO. \qquad (3)$$

Table 5. Multiple Regression Models Using Data From 1963 to 2010 and Their Statistics[a]

	Intercept	NAO	Nino3.4	Nino3.4^2	NAO·Nino3.4^2	NAO·Nino3.4	Residual Standard Error	R^2	Adjusted R^2	F Test
Model 1							0.89	0.26	0.21	
Coefficient	0.35	−0.15	−0.16	−0.35	–	–				**5.16**
T value	1.96	−1.07	−1.25	−2.86	–	–				
Probability	0.056	0.290	0.220	0.006	–	–				0.0038
SE	0.18	0.14	0.13	0.12	–	–				
Variance/Total Variance		6.8	5.47	13.75	–	–				
Model 2							0.86	0.34	0.27	
Coefficient	0.40	−0.45	−0.12	−0.50	0.28	–				**5.43**
T value	2.34	−2.37	−0.92	−3.69	2.21	–				
Probability	0.024	0.022	0.36	0.00063	0.032	–				0.0013
SE	0.17	0.19	0.13	0.14	0.13	–				
Variance/Total Variance		6.8%	4.7%	13.75%	7.53%	–				
Model 3							0.87	0.34	0.26	
Coefficient	0.40	−0.44	0.13	−0.49	0.27	0.033				**4.26**
T value	2.27	−2.27	−0.94	−3.41	1.98	0.26				
Probability	0.029	0.028	0.35	0.0014	0.054	0.79				0.0032
SE	0.18	0.20	0.14	0.14	0.14	0.13				
Variance/Total Variance		6.8%	7.6%	12.22%	6.18%	0.85%				
Model 4							0.97	0.12	0.08	
Coefficient	5.78e-05	−0.27	−0.23	–	–	–				3.15
T value	0.0004	−1.93	−1.68	–	–	–				
Probability	1.00	0.060	0.100	–	–	–				0.0520
SE	0.14	0.14	0.14	–	–	–				
Variance/Total Variance		6.8%	5.47%	–	–	–				
Model 5							0.90	0.23	0.20	
Coefficient	0.38	−0.13	–	−0.38	–	–				**6.88**
T value	2.12	−0.95	–	−3.12	–	–				
Probability	0.039	0.35	–	0.003	–	–				0.0025
SE	0.18	0.14	–	0.12	–	–				
Variance/Total Variance		6.8%	–	16.61%	–	–				

[a]The smaller the standard residual error, the better the hindcast model. The higher the adjusted R^2 value, the better the correlation between the hindcast model and the observed ice time series. The higher the overall F test, the better the regression model. Bold font indicates that the F test is significant at the 95% level. SE, standard error.

[47] The correlation between observations and estimates by the linear model (equation (3)) is only 0.35, although it is significant at the 95%, but not 99%, confidence level. The severe ice maxima and minima are poorly captured (figure not shown). The overall F test is not significant at the 95% confidence level (F = 3.15, Pr = 0.052, see Table 5, model 4)

[48] Based on the discussion in section 3, which includes r(NAO, ice) = 0.27, r(NAO^2, ice) = 0.10, r(Nino3.4, ice) =
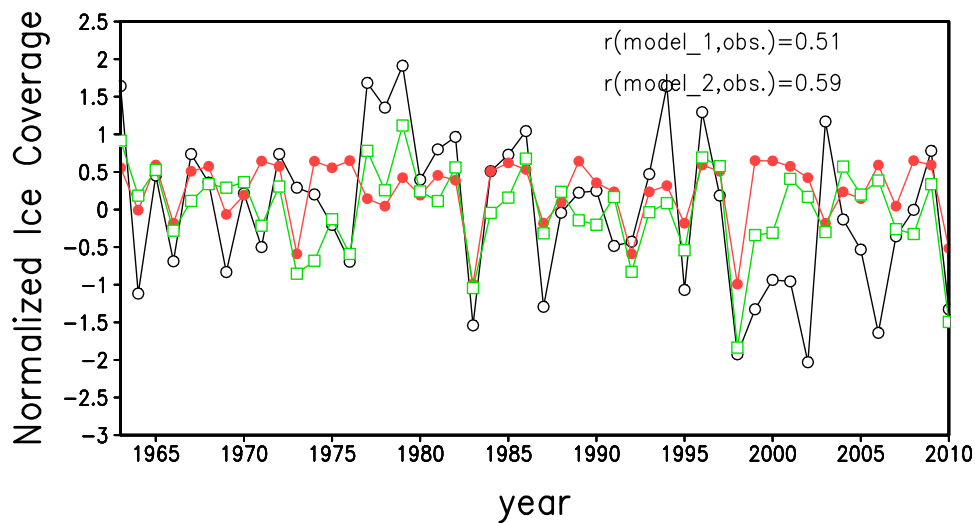
Figure 13. Modeled and observed normalized ice coverage for 1963–2010. Black is observations; red is estimated by regression model with the Nino3.4 index, quadratic Nino3.4 index, and the NAO index as predictors; while green is estimated by regression model with Nino3.4 index, quadratic Nino3.4 index, NAO index, and NAO·Nino3.4^2 as predictors. The correlation coefficients are r(model_1,obs.) = 0.51, r(model_2,obs.) = 0.59.
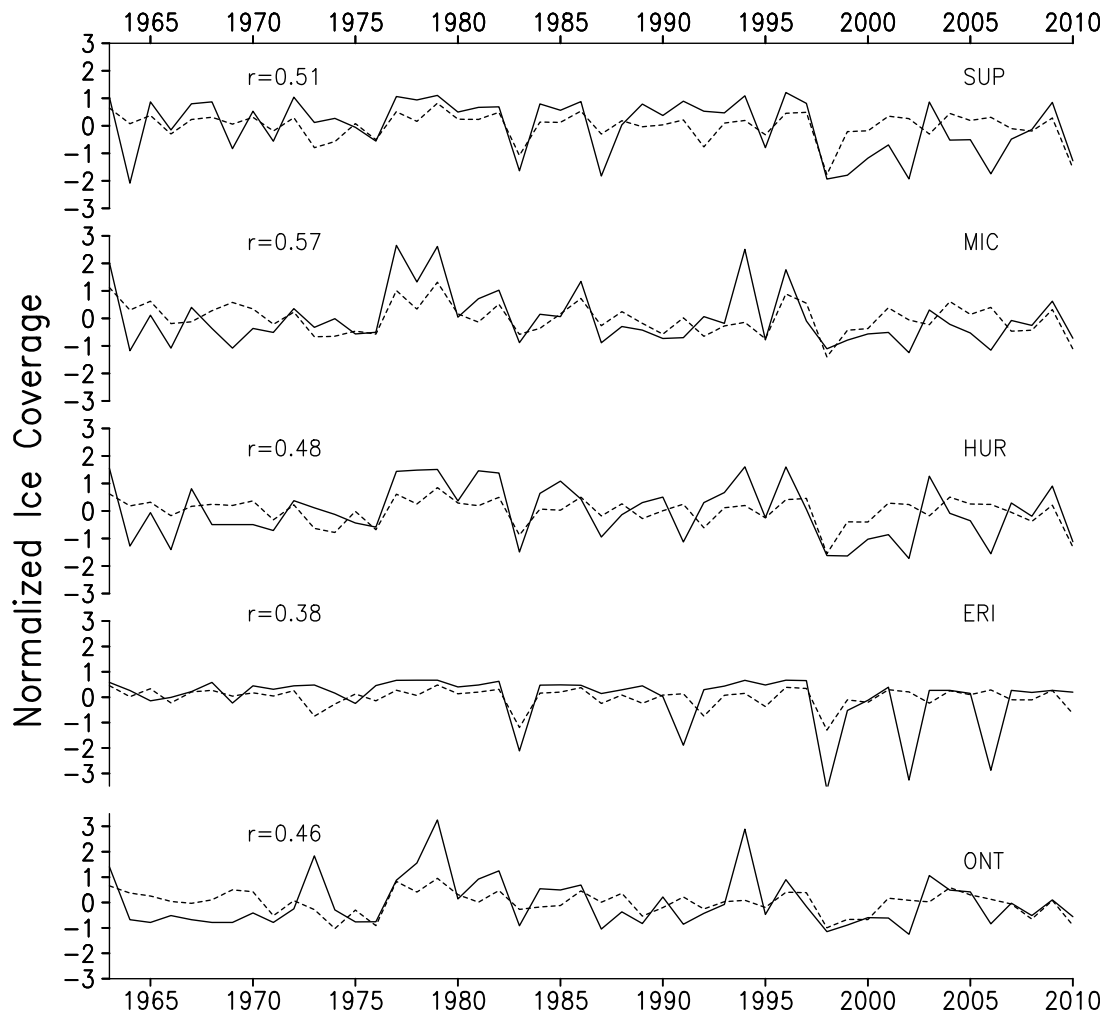
Figure 14. Modeled (dashed line) and observed (solid line) normalized AMIC of five lakes for the period 1963–2010. The correlations between modeled and observed are also shown.

−0.22, and r(Nino3.4^2, ice) = −0.48, we further included the quadratic form of the Nino3.4 index to obtain the hindcast model:

$$y = 0.35 − 0.16Nino3.4 − 0.35Nino3.4^2 − 0.15NAO. \quad (4)$$

[49] The corresponding graph is shown in Figure 13 along with observations. The correlation between observed and hindcasted time series by the nonlinear model (equation (4)) increases to 0.51 (R^2 = 0.26), which is significant at the 99% confidence level. The adjusted R^2 value is 0.21. The overall *F* test is significant at the 99% level (F = 5.16, Pr = 0.0038) (Table 5, model 1). It is obvious that including Nino3.4^2 significantly improves the prediction of Great Lakes ice cover.

[50] To address the importance of the nonlinear effect of ENSO on lake ice, an additional regression model:

$$y = 0.38 − 0.38Nino3.4^2 − 0.13NAO \quad (5)$$

was constructed with only two terms: NAO index and quadratic form of Nino3.4 index. The overall adjusted R^2 value (0.2) is just slightly smaller than the nonlinear model (model

1, equation (4)), indicating the quadratic (nonlinear) effect of ENSO is more important than its linear effect. We also constructed a regression model using both linear and quadratic terms of both the NAO and Nino3.4 indices; the adjusted R^2 value is 0.22, which is almost the same as 0.21 in model 2. In other words, adding the quadratic form of NAO index into the regression model does not significantly improve the prediction.

[51] To include the interference effects of NAO and ENSO as discussed in section 4, we add two predictors in the model: one is the product of NAO and quadratic form of Nino3.4 index; the other is the product of NAO and Nino3.4 index.

[52] When the interactive term NAO × Nino3.4^2 is included, the model is expressed as:

$$y = 0.40 − 0.12Nino3.4 − 0.50Nino3.4^2 − 0.45NAO$$

$$+ 0.28NAO·Nino3.4^2. \quad (6)$$

[53] The overall correlation and F value increases to 0.59 and 5.4, respectively, both are significant at 99% confidence level. The adjusted R^2 value is 0.274. In this model, except

Table 6. Multiple Regression Models for Five Lakes Using Data From 1963 to 2010 and Their Statistics[a]

	Intercept	NAO	Nino3.4	Nino3.4^2	NAO·Nino3.4^2	Residual Standard Error	R^2	Adjusted R^2	F Test
Superior						0.91	0.27	0.20	
Coefficient	0.40	−0.27	−0.13	−0.47	0.22				**3.9**
T value	2.18	−1.33	−1.0	−3.30	1.62				
Probability	0.035	0.19	0.32	0.0020	0.11				0.0089
SE	0.18	0.20	0.14	0.14	0.13				
Variance/Total Variance		2.13%	5.81%	14.08%	4.50%				
Michigan						0.87	0.32	0.26	
Coefficient	0.29	−0.65	−0.058	−0.41	0.33				**5.1**
T value	1.68	−3.4	−0.44	−2.97	2.59				
Probability	0.1	0.0016	0.66	0.0048	0.013				0.0019
SE	0.17	0.19	013	0.14	0.13				
Variance/Total Variance		13.25%	2.5%	5.88%	10.54%				
Huron						0.92	0.23	0.16	
Coefficient	0.40	−0.29	−0.022	−0.47	0.22				**3.30**
T value	2.15	−1.43	−0.16	−3.25	1.60				
Probability	0.037	0.16	0.87	0.0023	0.12				0.019
SE	0.19	0.20	0.14	0.15	0.14				
Variance/Total Variance		3.05%	1.66%	14.22%	4.53%				
Erie						0.98	0.15	0.068	
Coefficient	0.26	−0.13	−0.16	−0.28	0.052				1.86
T value	1.35	−0.60	−1.11	−1.8	0.36				
Probability	0.18	0.56	0.27	0.074	0.72				0.14
SE	0.20	0.22	0.15	0.15	0.14				
Variance/Total Variance		2.35%	4.86%	7.28%	0.26%				
Ontario						0.94	0.22	0.14	
Coefficient	0.34	−0.41	0.17	−0.42	0.26				**2.96**
T value	1.80	−1.99	1.18	−2.88	1.85				
Probability	0.080	0.053	0.24	0.0062	0.071				0.03
SE	0.19	0.21	0.14	0.15	0.14				
Variance/Total Variance		5.62%	0.43%	9.27%	6.25%				

[a]The smaller the standard residual error, the better the hindcast model. The higher the adjusted R^2 value, the better the correlation between the hindcast model and the observed ice time series. The higher the overall F test, the better the regression model. Bold font indicates that the F test is significant at the 95% level. SE, standard error.

Nino3.4, the t value of all other predictors is significant at 95% confidence level (Table 5, model 2). The statistic summary indicates that including the product of NAO and quadratic Nino3.4 remarkably improves the prediction. Some ice maxima and minima are better captured than the model 1 (Figure 13, green line).

[54] We further included the product of NAO and Nino3.4 and obtained the model:

$$y = 0.40 - 0.13 Nino3.4 - 0.49 Nino3.4^2 - 0.44 NAO$$
$$+ 0.27 NAO \cdot Nino3.4^2 - 0.033 NAO \cdot Nino3.4 \quad (7)$$

[55] The R^2 of this model (0.3366) is almost the same as model 2 (equation (6), $R^2 = 0.3356$), but both the adjusted R^2 and F value are slightly smaller than model 2. The estimated coefficient for NAO × Nino3.4 is very small (−0.033). These statistics suggest that the interactive term NAO × Nino3.4 has little effect on the prediction of Great Lakes ice cover.

[56] The comparison of the hindcast models revealed that the model 2 (equation (5)) is the best model for the Great Lakes ice cover. The model includes the linear effects of NAO and ENSO, the nonlinear effect of ENSO, and the interactive term NAO × Nino3.4^2.

[57] The fitting model for each lake was then constructed with the same predictors as model 2.

$$y_{Sup} = 0.40 - 0.13 Nino3.4 - 0.47 Nino3.4^2 - 0.27 NAO$$
$$+ 0.22 NAO \cdot Nino3.4^2, \quad (8)$$

$$y_{Mic} = 0.29 - 0.058 Nino3.4 - 0.41 Nino3.4^2 - 0.65 NAO$$
$$+ 0.33 NAO \cdot Nino3.4^2, \quad (9)$$

$$y_{Hur} = 0.40 - 0.02 Nino3.4 - 0.47 Nino3.4^2 - 0.29 NAO$$
$$+ 0.22 NAO \cdot Nino3.4^2, \quad (10)$$

$$y_{Eri} = 0.26 - 0.16 Nino3.4 - 0.28 Nino3.4^2 - 0.13 NAO$$
$$+ 0.052 NAO \cdot Nino3.4^2, \quad (11)$$

$$y_{Ont} = 0.34 - 0.17 Nino3.4 - 0.43 Nino3.4^2 - 0.41 NAO$$
$$+ 0.26 NAO \cdot Nino3.4^2. \quad (12)$$

[58] The corresponding graphs are shown in Figure 14 along with observations. The statistics of the models are listed in Table 6. The F test indicates that except Lake Erie, the models for all other lakes are significant at the 95% level. The model for Lake Michigan has the highest skill, while the model for Lake Erie has the lowest skill.
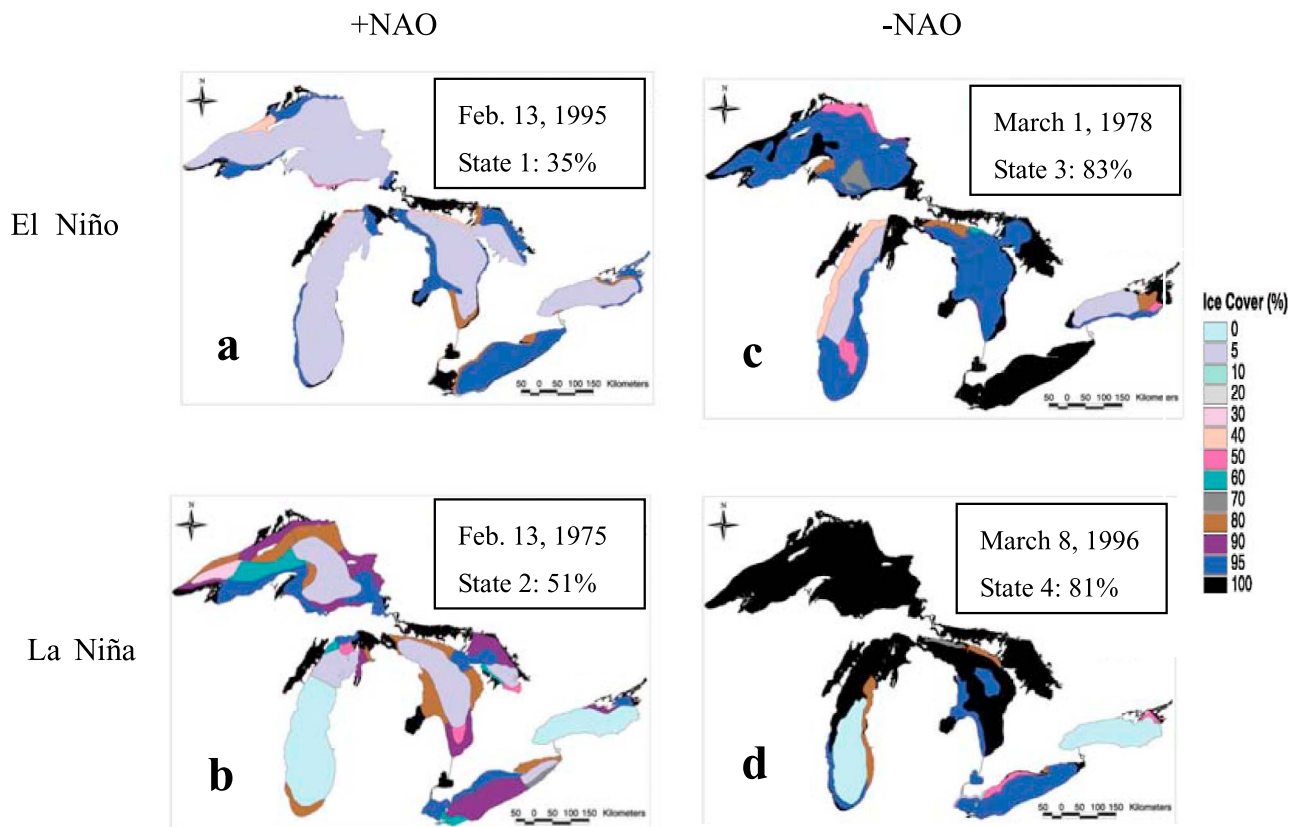
Figure 15. Least ice winter of 1995 (AMIC = 35%) during simultaneous El Niño and +NAO events ((a) state 1) and severe ice winter of 1996 (AMIC = 81%) during the simultaneous La Niña and −NAO events ((d) state 4). The maximum ice cover was 35% and 81%, respectively, significantly different from the climatology of 55%. During states (b) 2 and (c) 3, AMIC was 51% and 83%, respectively, in the winters of 1975 and 1978.

[59] This suggests that using the quadratic form of the Nino3.4 index instead of the Nino3.4 index only can significantly improve the prediction skill of Great Lakes ice cover. Including the interactive term NAO × Nino3.4^2 can further improve the prediction skill, and the ice maxima and minima are better, but still not very well captured. This implies that severe ice conditions are not well revealed by the linear regression model, although improved by the nonlinear model, because the action centers of both NAO and ENSO are displaced from year to year. Thus, the Great Lakes, which are geographically located on the edge of two important PNA action centers and on the southwestern edge of the Icelandic Low, display a very complicated regional response to two major climate patterns. Thus, case study is very important to reveal extreme ice conditions caused by displacement of the action centers [*Wang et al.*, 2010; *Bai et al.*, 2011].

6. Case Study

[60] Extreme ice conditions (maxima and minima) occurred in the Great Lakes from time to time in response to extreme weather events that are controlled by large-scale teleconnection climate patterns. To demonstrate the in-phase forcing by both NAO and ENSO on lake ice, we chose the two years 1995 and 1996, which fall into climate

states 1 and 4, respectively. We also chose 1975 and 1978 as the representatives of states 2 and 3 (see Table 2), in which competition between the two patterns occurs.

[61] Based on the above investigation, the rule of the thumb is that climate states 1 and 4 are the warm and cold years, respectively, which have relatively higher predictability skills for lake ice than climate states 2 and 3. The reason is that the +NAO (warm) and La Niña (cold) effects usually compete with each other under climate state 2, depending on which forcing is stronger; so do the −NAO (cold) and El Niño (warm) under climate state 3. Thus, case-to-case studies are essential in the projection of Great Lakes ice conditions during climate states 2 and 3.

[62] To demonstrate the combined effects of NAO and ENSO, we chose climate states 1 and 4 because lake ice during these two states has relatively higher predictability. During the simultaneous occurrence of +NAO and El Niño in the 1995 winter, lake ice maximum extent was only 35.1% (Figure 15a). On 13 February 1995, the annual maximum ice chart shows that except in Lake Erie, the shallowest lake in all five lakes, where the ice cover was above 95%; the other four lakes had about 5% ice coverage except along the coast. Even Lake Superior, the northernmost lake, had 5% ice coverage for most of the area except along the coast. As discussed above, the +NAO and ENSO simultaneously produced the in-phase positive SAT

anomalies over the Great Lakes (Figure 11a), leading to this extreme event.

[63] During the simultaneous occurrence of −NAO and La Niña (state 4), lake ice maximum extent was 81% (Figure 15d). On 8 March 1996, the annual maximum ice chart shows that most of the Great Lakes were covered by ice, except in southern Lake Michigan and Lake Ontario. In particular, Lake Superior was completely ice covered with ice concentration at 100%. This in-phase −NAO and La Niña events produced the extremely cold SAT (Figure 11d), leading to the extreme ice cover. Thus, the combined effect of NAO and ENSO possesses a relatively higher predictability skill under climate states 1 and 4 for long-term lake ice variability than individual indices (see Table 4).

[64] Annual maximum ice concentration was 51% on 13 February 1975, during the simultaneous +NAO and La Niña (state 2, Figure 15b), close to the climatology (54.5%). This case indicates the cancellation between the warming induced by the +NAO event and the cooling induced by the La Niña event in the Great Lakes.

[65] On 1 March 1978, the Great Lakes experienced heavy ice cover with a maximum concentration being 83% during the simultaneous −NAO and El Niño events (Figure 15c). Since the El Niño event was weaker than the NAO event (Nino3.4 index was 0.5°C, and the NAO index was −1.0), the −NAO dominated over the El Niño event, leading to a cold winter in the Great Lakes region. This case indicates the competition between these two climate patterns.

7. Conclusions and Summary

[66] The impacts of NAO and ENSO on Great Lakes ice cover were investigated using lake ice observations for winters 1963–2010 and NCEP reanalysis data. The following conclusions can be drawn.

[67] 1. Both NAO and ENSO impact Great Lakes ice cover. The Great Lakes tend to have lower (higher) ice cover during the positive (negative) NAO. Negative NAO coincides with 8 out of 14 maximal ice cover winters. El Niño events are often associated with below-normal ice cover: there were 12 lower ice cover winters out of 17 El Niño events during the period 1963–2010. Strong El Niño events can lead to minimal ice cover: 7 out of 10 strong El Niño events had minimal ice cover, which accounts for about half (47%) of total 15 minimal ice cover winters. The influence of La Niña on Great Lakes ice cover is intensity-dependent: the Great Lakes tend to have lower (higher) than normal ice cover during strong (weak) La Niña events. The interference of these two forcings complicates the relationship between ice coverage and NAO, and ENSO.

[68] 2. The nonlinear and asymmetric effects of ENSO on Great Lakes ice cover are important in addition to NAO effects. Although the correlation between the Nino3.4 index and ice coverage (−0.22) is not significant, the correlation coefficient between the quadratic term of Nino3.4 index and ice coverage (−0.48) turns out to be significant at the 99% confidence level. This asymmetric response of Great Lakes ice cover to ENSO is mainly due to the phase shift of the teleconnection patterns caused by convection anomalies shift during the opposite phases of ENSO. The interface of NAO influence might also contribute to the asymmetric response, which needs to be investigated further. The

relationship between the NAO index and lake ice cover is basically linear (r = 0.27), while the correlation between the square of NAO index and lake ice is only 0.10. Based on these findings, multiple-variable nonlinear regression models were developed for predicting ice coverage using Nino3.4 index, the quadratic Nino3.4 index, the NAO index, and the interactive term NAO × Nino3.4^2 as predictors. Using Nino3.4^2 instead of the index itself (linear model: r = 0.35 at the 95% significance level) can significantly improve the prediction of Great Lakes Ice cover (r = 0.51 at the 99% significance level). Including the interactive term further improves the prediction skill (the correlation increases from 0.51 to 0.59).

[69] 3. Four major climate states can be defined to predict ice conditions in the Great Lakes: (1) +NAO/El Niño, (2) +NAO/La Niña, (3) −NAO/El Niño, and (4) −NAO/La Niña. Generally speaking, ice conditions during climate states 1 (mild ice cover) and 4 (severe ice cover) have higher predictability skills than climate states 2 and 3. The combined indices of NAO and ENSO possess higher predictability skill for long-term ice variability than individual index.

[70] 4. Case study is essential in studies of ice conditions during climate states 2 and 3 due to the low predictability skill, since the competition effects occur between the +NAO (warm) and La Niña (cold), and between −NAO (cold) and El Niño (warm), depending on which forcing is stronger. There are scenarios that indicate that one climate pattern dominated over the other, such as on 1 March 1978 (state 3). Due to the location of the Great Lakes that are located on the edge of the action centers of the two internal climate patterns, PNA and NAO, case studies need to be conducted for climate states 2 and 3 to better understand the lake ice change in response to the climate forcing and the changes in intensity and location of the action centers.

References

Anderson, W. L., D. M. Robertson, and J. J. Magnuson (1996), Evidence of recent warming and El Niño–related variations in ice break-up of Wisconsin lakes, *Limnol. Oceanogr.*, *41*, 815–821, doi:10.4319/lo. 1996.41.5.0815.

Assel, R. A., and D. M. Robertson (1995), Changes in winter air temperatures near Lake Michigan during 1851–1993, as determined from regional lake-ice records, *Limnol. Oceanogr.*, *40*, 165–176, doi:10.4319/lo. 1995.40.1.0165.

Assel, R. A., and S. Rodionov (1998), Atmospheric teleconnections for annual maximal ice cover on the Laurentian Great Lakes, *Int. J. Climatol.*, *18*, 425–442, doi:10.1002/(SICI)1097-0088(19980330)18:4<425:: AID-JOC258>3.0.CO;2-Q.

Assel, R. A., K. Cronk, and D. C. Norton (2003), Recent trends in Laurentian Great Lakes ice cover, *Clim. Change*, *57*, 185–204, doi:10.1023/ A:1022140604052.

Assel, R. A., F. H. Quinn, and C. E. Sellinger (2004), Hydro-climatic factors of the recent drop in Laurentian Great Lakes water levels, *Bull. Am. Meteorol. Soc.*, *85*, 1143–1151, doi:10.1175/BAMS-85-8-1143.

Bai, X., J. Wang, C. Sellinger, A. Clites, and R. Assel (2010), The impacts of ENSO and AO/NAO on the interannual variability of Great Lakes ice cover, *Tech. Memo. GLERL-152*, 44 pp., Great Lakes Environ. Res. Lab., NOAA, Ann Arbor, Mich.

Bai, X., J. Wang, Q. Liu, D. Wang, and Y. Liu (2011), Severe ice conditions in the Bohai Sea, China and mild ice conditions in the Great Lakes during the 2009/2010 winter: Links to El Nino and a strong negative Arctic Oscillation, *J. Appl. Meteorol. Climatol.*, *50*, 1922–1935, doi:10.1175/2011JAMC2675.1.

Barnston, A. G. (1994), Linear statistical short-term climate predictive skill in the Northern Hemisphere, *J. Clim.*, *7*, 1513–1564, doi:10.1175/1520-0442(1994)007<1513:LSSTCP>2.0.CO;2.

Barnston, A. G., and R. E. Livezey (1987), Classification, seasonality and persistence of low-frequency atmospheric circulation patterns, *Mon. Weather Rev.*, *115*, 1083–1126, doi:10.1175/1520-0493(1987)115<1083:CSAPOL>2.0.CO;2.

Bilello, M. A. (1980), Maximum thickness and subsequent decay of lake, river and fast sea ice in Canada and Alaska, *Rep. 80–6*, U.S. Army Cold Reg. Res. and Eng. Lab., Hanover, N. H.

Bonsal, B. R., T. D. Prowse, C. R. Duguay, and M. P. Lacroix (2006), Impacts of large-scale teleconnections on lake ice duration over Canada, *J. Hydrol.*, *330*, 340–353, doi:10.1016/j.jhydrol.2006.03.022.

Brown, L. C., and C. R. Duguay (2010), The response and role of ice cover in lake-climate interactions, *Prog. Phys. Geogr.*, *34*(5), 671–704, doi:10.1177/0309133310375653.

Brown, R., W. Taylor, and R. A. Assel (1993), Factors affecting the recruitment of lake whitefish in two areas of northern Lake Michigan, *J. Great Lakes Res.*, *19*, 418–428, doi:10.1016/S0380-1330(93)71229-0.

Derome, J., et al. (2001), Seasonal predictions based on two dynamical models, *Atmos. Ocean*, *39*, 485–501, doi:10.1080/07055900.2001.9649690.

Freund, J. E., and G. A. Simon (1992), *Modern Elementary Statistics*, 8th ed., 578 pp., Prentice Hall, Englewood Cliffs, N. J.

Gershunov, A., and T. P. Barnett (1998), ENSO influence on intraseasonal extreme rainfall and temperature frequencies in the contiguous United States: Observations and model results, *J. Clim.*, *11*, 1575–1586, doi:10.1175/1520-0442(1998)011<1575:EIOIER>2.0.CO;2.

Ghanbari, R. N., H. R. Bravo, J. J. Magnuson, W. G. Hyzer, and B. J. Benson (2009), Coherence between lake ice cover, local climate and teleconnections (Lake Mendota, Wisconsin), *J. Hydrol.*, *374*, 282–293, doi:10.1016/j.jhydrol.2009.06.024.

Halpert, M. S., and C. F. Ropelewski (1992), Surface temperature patterns associated with the Southern Oscillation, *J. Clim.*, *5*, 577–593, doi:10.1175/1520-0442(1992)005<0577:STPAWT>2.0.CO;2.

Hanson, P. H., C. S. Hanson, and B. H. Yoo (1992), Recent Great Lakes ice trends, *Bull. Am. Meteorol. Soc.*, *73*, 577–584, doi:10.1175/1520-0477(1992)073<0577:RGLIT>2.0.CO;2.

Hoerling, M. P., A. Kumar, and M. Zhong (1997), El Niño, La Niña and the nonlinearity of their teleconnections, *J. Clim.*, *10*, 1769–1786, doi:10.1175/1520-0442(1997)010<1769:ENOLNA>2.0.CO;2.

Hoerling, M. P., A. Kumar, and T. Xu (2001), Robustness of the nonlinear climate response to ENSO's extreme phases, *J. Clim.*, *14*, 1277–1293, doi:10.1175/1520-0442(2001)014<1277:ROTNCR>2.0.CO;2.

Horel, J. D., and J. M. Wallace (1981), Planetary-scale atmospheric phenomena associated with the Southern Oscillation, *Mon. Weather Rev.*, *109*, 813–829, doi:10.1175/1520-0493(1981)109<0813:PSAPAW>2.0.CO;2.

Kalnay, E., et al. (1996), The NCEP/NCAR 40-year reanalysis project, *Bull. Am. Meteorol. Soc.*, *77*, 437–471, doi:10.1175/1520-0477(1996)077<0437:TNYRP>2.0.CO;2.

Kiladis, G. N., and H. F. Diaz (1989), Global climatic anomalies associated with extremes in the Southern Oscillation, *J. Clim.*, *2*, 1069–1090, doi:10.1175/1520-0442(1989)002<1069:GCAAWE>2.0.CO;2.

Lau, N. C., and M. J. Nath (1990), A general circulation model study of the atmospheric response to extratropical SST anomalies observed in 1950–1979, *J. Clim.*, *3*, 965–989, doi:10.1175/1520-0442(1990)003<0965:AGCMSO>2.0.CO;2.

Livezey, R. E., A. Leetmaa, M. Mautani, H. Rui, M. Ji, and A. Kumar (1997), Teleconnective response of the Pacific–North American region atmosphere to large central equatorial Pacific SST anomalies, *J. Clim.*, *10*, 1787–1820, doi:10.1175/1520-0442(1997)010<1787:TROTPN>2.0.CO;2.

Livingstone, D. M. (2000), Large-scale climatic forcing detected in historical observations of lake ice break-up, *Verh. Int. Ver. Theor. Angew. Limnol.*, *27*, 2775–2783.

Magnuson, J., et al. (1995), Region 1: Laurentian Great Lakes and Precambrian Shield, paper presented at Regional Assessment of Freshwater Ecosystems and Climate Change in North America, Am. Soc. of Limnol. and Oceanogr., Leesburg, Va.

Magnuson, J. J., et al. (2000), Historical trends in lake and river ice cover in the Northern Hemisphere, *Science*, *289*, 1743–1746, doi:10.1126/science.289.5485.1743.

Mishra, V., K. A. Cherkauer, L. C. Bowling, and M. Huber (2011), Lake ice phenology of small lakes: Impacts of climate variability in the Great Lakes region, *Global Planet. Change*, *76*, 166–185, doi:10.1016/j.gloplacha.2011.01.004.

Mo, K. C., and R. E. Livezey (1986), Tropical-extratropical geopotential height teleconnections during the Northern Hemisphere winter, *Mon. Weather Rev.*, *114*, 2488–2515, doi:10.1175/1520-0493(1986)114<2488:TEGHTD>2.0.CO;2.

Mysak, L. A., R. G. Ingram, J. Wang, and A. van der Baaren (1996), Anomalous sea-ice extent in Hudson Bay, Baffin Bay and the Labrador Sea during three simultaneous ENSO and NAO episodes, *Atmos. Ocean*, *34*, 313–343, doi:10.1080/07055900.1996.9649567.

Niimi, A. J. (1982), Economic and environmental issues of the proposed extension of the winter navigation season and improvements on the Great Lakes–St. Lawrence Seaway system, *J. Great Lakes Res.*, *8*, 532–549, doi:10.1016/S0380-1330(82)71991-4.

Palecki, M. A., and R. G. Barry (1986), Freeze-up and break-up of lakes as an index of temperature changes during the transition seasons: A case study in Finland, *J. Clim. Appl. Meteorol.*, *25*, 893–902, doi:10.1175/1520-0450(1986)025<0893:FUABUO>2.0.CO;2.

Qian, S. (2009), *Environmental and Ecological Statistics With R*, 420 pp., Chapman and Hall, Boca Raton, Fla.

Robertson, D. M., R. H. Wynne, and W. Y. B. Chang (2000), Influence of El Niño on lake and river ice cover in the Northern Hemisphere from 1900 to 1995, *Verh. Int. Ver. Theor. Angew. Limnol.*, *27*, 2784–2788.

Rodionov, S., and R. A. Assel (2000), Atmospheric teleconnection patterns and severity of winters in the Laurentian Great Lakes basin, *Atmos. Ocean*, *38*, 601–635, doi:10.1080/07055900.2000.9649661.

Rodionov, S., and R. A. Assel (2001), A new look at the Pacific/North American index, *Geophys. Res. Lett.*, *28*, 1519–1522, doi:10.1029/2000GL012185.

Rodionov, S., and R. A. Assel (2003), Winter severity in the Great Lakes region: A tale of two oscillations, *Clim. Res.*, *24*, 19–31, doi:10.3354/cr024019.

Rodionov, S., R. A. Assel, and L. R. Herche (2001), Tree-structured modeling of the relationship between Great Lakes ice cover and atmospheric circulation patterns, *J. Great Lakes Res.*, *27*, 486–502, doi:10.1016/S0380-1330(01)70662-4.

Rogers, J. C. (1984), The association between the North Atlantic Oscillation and the Southern Oscillation in the Northern Hemisphere, *Mon. Weather Rev.*, *112*, 1999–2015, doi:10.1175/1520-0493(1984)112<1999:TABTNA>2.0.CO;2.

Ropelewski, C. F., and M. S. Halpert (1986), North American precipitation and temperature patterns associated with the El Niño Southern Oscillation (ENSO), *Mon. Weather Rev.*, *114*, 2352–2362, doi:10.1175/1520-0493(1986)114<2352:NAPATP>2.0.CO;2.

Shabbar, A., and A. G. Barnston (1996), Skill of seasonal forecasts in Canada using canonical correlation analysis, *Mon. Weather Rev.*, *124*, 2370–2385, doi:10.1175/1520-0493(1996)124<2370:SOSCFI>2.0.CO;2.

Smith, J. B. (1991), The potential impacts of climate change on the Great Lakes, *Bull. Am. Meteorol. Soc.*, *72*, 21–28, doi:10.1175/1520-0477(1991)072<0021:TPIOCC>2.0.CO;2.

Thompson, D. W. J., and J. M. Wallace (1998), The Arctic Oscillation signature in the wintertime geopotential height and temperature fields, *Geophys. Res. Lett.*, *25*, 1297–1300, doi:10.1029/98GL00950.

Trenberth, K. E., G. W. Branstator, D. Karoly, A. Kumar, N.-C. Lau, and C. Ropelewski (1998), Progress during TOGA in understanding and modeling global teleconnections associated with tropical sea surface temperatures, *J. Geophys. Res.*, *103*, 14291–14324, doi:10.1029/97JC01444.

Vanderploeg, H. A., S. J. Bolsenga, G. L. Fahnenstiel, J. R. Liebig, and W. S. Gardner (1992), Plankton ecology in an ice-covered bay of Lake Michigan: Utilization of a winter phytoplankton bloom by reproducing copepods, *Hydrobiologia*, *243–244*, 175–183, doi:10.1007/BF00007033.

Wallace, J. M., and D. Gutzler (1981), Teleconnection in the geopotential height field during the Northern Hemisphere winter, *Mon. Weather Rev.*, *109*, 784–812, doi:10.1175/1520-0493(1981)109<0784:TITGHF>2.0.CO;2.

Wallace, J. M., and Q. Jiang (1992), On the observed structure of the interannual variability of the atmosphere/ocean climate system, in *Atmospheric and Oceanic Variability*, edited by H. Cattle, pp. 17–43, R. Meteorol. Soc., Bracknell, U. K.

Wallace, J. M., C. Smith, and Q. Jiang (1990), Spatial patterns of atmosphere-ocean interaction in the northern winter, *J. Clim.*, *3*, 990–998, doi:10.1175/1520-0442(1990)003<0990:SPOAOI>2.0.CO;2.

Wallace, J. M., C. Smith, and C. S. Bretherton (1992), Singular value decomposition of wintertime sea surface temperature and 500-mb

height anomalies, *J. Clim.*, *5*, 561–576, doi:10.1175/1520-0442(1992) 005<0561:SVDOWS>2.0.CO;2.

Wang, J., and M. Ikeda (2000), Arctic oscillation and Arctic sea-ice oscillation, *Geophys. Res. Lett.*, *27*, 1287–1290, doi:10.1029/1999GL002389.

Wang, J., L. A. Mysak, and R. G. Ingram (1994), Interannual variability of sea-ice cover in Hudson Bay, Baffin Bay and the Labrador Sea, *Atmos. Ocean*, *32*, 421–447, doi:10.1080/07055900.1994.9649505.

Wang, J., M. Ikeda, S. Zhang, and R. Gerdes (2005), Linking the Northern Hemisphere sea ice reduction trend and the quasi-decadal Arctic sea ice oscillation, *Clim. Dyn.*, *24*, 115–130, doi:10.1007/s00382-004-0454-5.

Wang, J., X. Bai, G. Leshkevich, M. Colton, A. Clites, and B. Lofgren (2010), Severe Great Lakes ice cover in winter 2008–2009, *Eos Trans. AGU*, *91*(5), 41–42, doi:10.1029/2010EO050001.

Wang, J., X. Bai, H. Hu, A. Clites, M. Colton, and B. Lofgren (2012), Temporal and spatial variability of Great Lakes ice cover, 1973–2010, *J. Clim.*, *25*, 1318–1329, doi:10.1175/2011JCLI4066.1.

Williams, G. P. (1965), Correlating freeze-up and break-up with weather conditions, *Can. Geotech. J.*, *2*, 313–326, doi:10.1139/t65-047.

Wu, A., W. W. Hsieh, and A. Shabbar (2005), The nonlinear patterns of North American winter temperature and precipitation associated with ENSO, *J. Clim.*, *18*, 1736–1752, doi:10.1175/JCLI3372.1.

Zwiers, F. (1987), A potential predictability study conducted with an atmospheric general circulation model, *Mon. Weather Rev.*, *115*, 2957–2974, doi:10.1175/1520-0493(1987)115<2957:APPSCW>2.0.CO;2.

R. Assel, A. Clites, and J. Wang, Great Lakes Environmental Research Laboratory, NOAA, 4840 S. State Rd., Ann Arbor, MI 48108, USA. (jia. wang@noaa.gov)

X. Bai, Cooperative Institute for Limnology and Ecosystems Research, University of Michigan, 4840 S. State Rd., Ann Arbor, MI 48108, USA.

C. Sellinger, College of Oceans and Atmospheric Sciences, Oregon State University, 104 COAS Admin Bldg., Corvallis, OR 97331-5503, USA.